

# Towards understanding epoch-wise double descent in two-layer linear neural networks

Amanda Olmin, Fredrik Lindsten  
Linköping University, Sweden

## Abstract

Epoch-wise double descent is the phenomenon where generalisation performance improves beyond the point of overfitting, resulting in a generalisation curve exhibiting two descents under the course of learning. Understanding the mechanisms driving this behaviour is crucial not only for understanding the generalisation behaviour of machine learning models in general, but also for employing conventional selection methods, such as the use of early stopping to mitigate overfitting. While we ultimately want to draw conclusions of more complex models, such as deep neural networks, a majority of theoretical conclusions regarding the underlying cause of epoch-wise double descent are based on simple models, such as standard linear regression. To start bridging this gap, we study epoch-wise double descent in two-layer linear neural networks. First, we derive a gradient flow for the linear two-layer model, that bridges the learning dynamics of the standard linear regression model, and the linear two-layer diagonal network with quadratic weights. Second, we identify additional factors of epoch-wise double descent emerging with the extra model layer, by deriving necessary conditions for the generalisation error to follow a double descent pattern. While epoch-wise double descent in linear regression has been attributed to differences in input variance, in the two-layer model, also the singular values of the input-output covariance matrix play an important role. This opens up for further questions regarding unidentified factors of epoch-wise double descent for truly deep models.

## 1 Introduction

The bias-variance trade-off implies a U-shaped generalisation error, as a function of model complexity. It suggests that generalisation will improve with an increasing model complexity only to a certain point, after which the model will show signs of overfitting, and from which it never recovers. The double descent phenomenon contradicts this idea, showcasing how generalisation performance can improve even beyond the point where the model perfectly fits the training data [4, 18], leading to a generalisation curve following a so called double descent pattern.

The double descent pattern in generalisation error has been observed not only with increasing model size, resulting in *model-wise* double descent, but also with the number of training epochs, when training models using iterative learning algorithms such as gradient descent, resulting in so-called *epoch-wise* double descent, see e.g. [3, 18]. While model-wise double descent has been studied extensively ([4, 1, 2, 9, 14, 8] to name a few), it typically involves understanding the asymptotic behaviour of models, assuming infinite training time. Meanwhile, epoch-wise double descent requires understanding the whole trajectory of learning.

Typically, epoch-wise double descent has been studied either mainly through empirical observation, e.g. [18], or through the theoretical analysis of simple models, such as linear regression [15, 21, 19] or the random feature model [6, 7]. On the one end, [18] connects epoch-wise double descent, similar to model-wise double descent, to the notion of *model capacity*, attributing the second descent to the model capacity exceeding the number of training samples. On the other end, [15, 19, 7] connect epoch-wise double descent to differences in speed of learning, describing the generalisation error as consisting of overlapping bias-variance trade-off curves, corresponding to fast- and slow-learned features. With this, the eigenvalues of the input covariance matrix is integral to the double descent phenomenon. Moreover, we do not need overparametrisation for the epoch-wise double descent pattern to emerge, something that is also consistent with earlier observations of the phenomenon, see e.g. [3]. However, as the basis for these analyses are models consisting of just one layer of learnable parameters, while findings are corroborated empirically for deeper models, this leaves an open-ended question of possibly unidentified factors causing epoch-wise double descent in deeper models.

Although [15] admittedly do also study double descent in a two-layer neural network with ReLU activation, the insights of [15] do not connect double descent in two-layer networks directly to the properties of the data, but rather the Jacobian of the network. Meanwhile, another line of work, studying the gradient dynamics of linear two-layer networks, indicate that the singular values of the input-output covariance matrix of the training data are important factors in determining the speed of learning in these models [20, 10, 17, 22]. This suggests another factor important to the double descent phenomenon in two-layer linear neural networks, which has not been attributed as a factor of double descent in single-layer models. However, so far, and to the best of our knowledge, this has not been studied explicitly.

In this paper, we aim to start bridging the gap between epoch-wise double descent in the single-layer linear regression model and multi-layer neural networks, by studying double descent in the two-layer linear neural network. While this model is indeed still linear, the training dynamics are, in contrast to the single-layer model, non-linear. Moreover, the benefits of studying linear models, is that we can obtain closed-form solutions for the training dynamics, at least in the case where weights are *decoupled*, such that they evolve independently within a transformed space that is defined by the training data. More importantly, it opens up for the possibility of directly connecting epoch-wise double

descent to properties of the training data.

For our purposes, we derive the gradient flow for a two-layer diagonal, or decoupled, neural network, similar to what was studied in [22], but with non-isotropic input, and with individual learning rates for the first and second layer. With our formulation, the standard (single-layer) linear regression model is a special case of the dynamics, and hence we can connect our findings also to this special case. For the two-layer decoupled linear neural network, we

- Derive the time-dependent generalisation error as a superposition of bias-variance curves corresponding to each weight in the decoupled dynamics, assuming that the true model is linear.
- Characterise the behaviour of each individual bias-variance trade-off curve, and use this to find a necessary condition for epoch-wise double descent.

Through this analysis, we identify additional factors of epoch-wise double descent in the two-layer model, not observed in the one-layer model, including a connection to the singular values of the input-output covariance matrix as well as an additional circumstance under which epoch-wise double descent is possible.

## 2 Preliminaries

We will consider the problem of predicting the target  $y \in \mathbb{R}^{1 \times d_y}$  given the input  $x \in \mathbb{R}^{1 \times d}$ , using a two-layer linear network with  $h$  hidden units

$$\begin{aligned}\hat{y}(x) &= xW^\top, \\ W &= W^{(2)}W^{(1)},\end{aligned}$$

where  $W^{(1)} \in \mathbb{R}^{h \times d}$  and  $W^{(2)} \in \mathbb{R}^{d_y \times h}$ .

We train the linear network on  $n$  training data points  $(x_i, y_i)$ ,  $i = 1, \dots, n$ , using Mean Squared Error (MSE). Let  $\mathbf{X} = [x_1, \dots, x_n]^\top \in \mathbb{R}^{n \times d}$  and  $\mathbf{y} = [y_1, \dots, y_n]^\top \in \mathbb{R}^{n \times d_y}$ . The MSE criterion is

$$\mathcal{L}(W) = \frac{1}{2n} \text{Tr}((\mathbf{y} - \mathbf{X}W^\top)^\top (\mathbf{y} - \mathbf{X}W^\top)). \quad (1)$$

Assuming small learning rates for each model layer,  $\eta_a, \eta_b \geq 0$ , we study the gradient flow

$$\frac{1}{\eta_a} \frac{d}{dt} W^{(1)} = \frac{1}{n} W^{(2)\top} (\mathbf{y}^\top \mathbf{X} - W \mathbf{X}^\top \mathbf{X}), \quad (2)$$

$$\frac{1}{\eta_b} \frac{d}{dt} W^{(2)} = \frac{1}{n} (\mathbf{y}^\top \mathbf{X} - W \mathbf{X}^\top \mathbf{X}) W^{(1)\top}, \quad (3)$$

resulting from training the two-layer linear network using gradient descent and MSE loss.

### 3 Theory

In what follows, we derive decoupled dynamics for the two-layer linear neural networks, acting as a bridge between the dynamics of the one-layer linear model and the decoupled two-layer model with quadratic weights, studied in e.g. [20, 10]. Then, we use these dynamics to study factors of epoch-wise double descent in two-layer linear networks.

#### 3.1 Decoupled dynamics of the two-layer linear network

As a first step towards understanding double descent in two-layer linear neural networks, we will study the generalisation behaviour of the decoupled dynamics considered in e.g. [20, 10, 17, 22]. While a common assumption is  $\mathbf{X}^\top \mathbf{X} = \mathbb{I}$ , i.e the input is isotropic (see e.g. [20, 17, 22]), we will instead assume non-isotropic input where the input data matrix,  $\mathbf{X}$ , has the singular value decomposition (SVD)

$$n^{-1/2} \mathbf{X} = U \Sigma^{1/2} V^\top.$$

Furthermore, we will assume that the input-output covariance matrix  $n^{-1} \mathbf{y}^\top \mathbf{X}$  share right singular vectors with  $n^{-1/2} \mathbf{X}$ , and has the SVD

$$\begin{aligned} n^{-1} \mathbf{y}^\top \mathbf{X} &= U^{(yx)} \Sigma^{(yx)1/2} V^{(yx)\top}, \\ V^{(yx)} &= V. \end{aligned}$$

Note that this assumption is similar to the one made in [10]. While [10] allow for the matrix  $\Sigma$  to be non-diagonal with the addition of a perturbation matrix  $B$ , we here aim for simplicity by assuming  $B = \mathbf{0}$ . We refer to [10] for results on how the perturbation matrix  $B$  might affect the final solution to the dynamics. Moreover, while our derivations in actuality only require that the matrices  $V$  and  $V^{(yx)}$  share columns, up to a reshuffling of the elements of  $\Sigma$ , see appendix A.1, we keep it simple by using  $V^{(yx)} = V$  in the main article. We note that for the rank of  $\mathbf{y}^\top \mathbf{X}$  we have  $\text{rank}(\mathbf{y}^\top \mathbf{X}) \leq \min(\text{rank}(\mathbf{y}), \text{rank}(\mathbf{X}))$ , and therefore  $\text{rank}(\mathbf{y}^\top \mathbf{X}) \leq \text{rank}(\mathbf{X}^\top \mathbf{X})$ .

Following e.g. [20, 10, 17, 22] we initialise weights using a *spectral* initialisation according to  $W(0) = U^{(yx)} Z(0) V^\top$ , where  $Z = Z^{(2)} Z^{(1)}$ , and with  $Z^{(1)} := W^{(1)} V$ ,  $Z^{(2)} := U^{(yx)\top} W^{(2)}$ . Then, we study the evolution of the synaptic weights  $Z^{(1)}, Z^{(2)}$

$$\begin{aligned} \frac{1}{\eta_a} \frac{d}{dt} Z^{(1)} &= Z^{(2)\top} (\Sigma^{(yx)1/2} - Z \Sigma), \\ \frac{1}{\eta_b} \frac{d}{dt} Z^{(2)} &= (\Sigma^{(yx)1/2} - Z \Sigma) Z^{(1)\top}. \end{aligned} \tag{4}$$

Observe that as  $U^{(yx)}, V$  are constant matrices, we will keep the relationship between  $W$  and  $Z$  throughout learning. Moreover, we follow [20, 10, 17, 22] and

decouple weights by selecting  $Z(0)$  to be diagonal, initialising the  $i^{\text{th}}$  column,  $\alpha^{(i)}$ , of  $Z^{(1)}$ , and the  $i^{\text{th}}$  row,  $\beta^{(i)\top}$ , of  $Z^{(2)}$  according to  $\alpha^i, \beta^i \propto r^{(i)}$ , with  $r^{(i)}$  a constant, unit vector. Importantly,  $r^{(i)}$ ,  $i = 1, \dots, \min(d, d_y)$  are orthogonal, i.e.  $r^{(i)} \cdot r^{(j)} = 0$  for  $i \neq j$ . Note that for an undercomplete hidden layer, with hidden dimension  $h < \min(d, d_y)$ , this necessarily limits the rank of  $Z$  to  $h$ . Hence, requiring that we initialise at least  $\min(d, d_y) - h$  diagonal elements of  $Z$  at 0, with  $\alpha^{(i)} = \beta^{(i)} = \mathbf{0}$ , the vector of zeroes. If instead  $h \geq \min(d, d_y)$ , we can initialise weights such that  $Z$  has full rank.

With the given initialisation,  $Z$  will remain diagonal, see e.g. [20] and appendix A.1, resulting in the decoupled two layer dynamics where weights along the diagonal evolve independently. In the decoupled dynamics, a single weight along the diagonal of  $Z$  can be described by  $z_i = \alpha^{(i)} \cdot \beta^{(i)} = a_i b_i$ , with scalar projections  $a_i = \alpha^{(i)} \cdot r^i, b_i = \beta^{(i)} \cdot r^i$  evolving as

$$\begin{aligned} \frac{1}{\eta_a} \frac{da_i}{dt} &= b(\lambda_i^{(yx)1/2} - \lambda_i a_i b_i), \\ \frac{1}{\eta_b} \frac{db_i}{dt} &= a_i(\lambda_i^{(yx)1/2} - \lambda_i a_i b_i). \end{aligned} \quad (5)$$

We let  $\lambda_i$  and  $\lambda_i^{(yx)1/2}$  be the  $i^{\text{th}}$  diagonal elements of  $\Sigma$  and  $\Sigma^{(yx)}$ , respectively. Observe that,  $\lambda_i, \lambda_i^{(yx)1/2} \geq 0$  by definition.

To obtain a gradient flow for the product  $z_i = a_i b_i$ , we again follow previous work, e.g. [22], and make use of conserved quantities of the dynamical system eq. (5). Namely, with the relaxed assumption of different learning rates, solutions to eq. (5) follow trajectories for which  $\eta_b a_i^2 - \eta_a b_i^2 = \gamma$ , for some constant  $\gamma$ , see appendix A.2. Then,

$$\frac{dz_i}{dt} = \sqrt{\gamma^2 + 4\eta^2 z_i^2} (\lambda_i^{(yx)1/2} - \lambda_i z_i), \quad (6)$$

This is an extension of the gradient flow studied in [22] with what is referred to as an asymmetric, spectral initialisation. Here, we extend the dynamics in [22] by allowing for different learning rates in the two layers as well as allowing  $\lambda_i$  to be separated from 1. We note that, in the writing of this manuscript, [16] published a similar gradient flow to ours with different learning rates in the two model layers. However, the gradient flow of [16] does not depend on a decoupling of the weights, and hence a solution to the dynamics is provided only in the special case  $h = 1$  and  $\lambda_i = 1$ . Here we provide a solution to the decoupled dynamics for a general  $h, \lambda_i$  when  $z_i(0) < \lambda_i^{(yx)1/2} / \lambda_i$ .

**Proposition 1** Consider  $z(t)$  initialised at  $z_i(0) < \lambda_i^{(yx)1/2} / \lambda_i$  and assume  $\lambda_i > 0$ . The solution to eq. (6) is

$$z_i(t) = \frac{C^2 \lambda_i^2 \lambda_i^{(yx)1/2} e^{2\sqrt{\gamma^2 \lambda_i^2 + 4\eta^2 \lambda_i^{(yx)}} t} - 2C\gamma^2 \lambda_i^2 e^{\sqrt{\gamma^2 \lambda_i^2 + 4\eta^2 \lambda_i^{(yx)}} t} - 4\gamma^2 \eta^2 \lambda_i^{(yx)1/2}}{\lambda_i \left( C^2 \lambda_i^2 e^{2\sqrt{\gamma^2 \lambda_i^2 + 4\eta^2 \lambda_i^{(yx)}} t} + 8C\eta^2 \lambda_i^{(yx)1/2} e^{\sqrt{\gamma^2 \lambda_i^2 + 4\eta^2 \lambda_i^{(yx)}} t} - 4\gamma^2 \eta^2 \right)},$$

with

$$C = \frac{\sqrt{(\gamma^2 \lambda_i^2 + 4\eta^2 \lambda_i^{(yx)}) (\gamma^2 + 4\eta^2 z_i(0)^2) + \gamma^2 \lambda_i + 4\eta^2 \lambda_i^{(yx)1/2} z_i(0)}}{\lambda_i (\lambda_i^{(yx)1/2} - \lambda_i z_i(0))}.$$

Moreover, provided that  $z_i(0) > 0$  in the special case  $\gamma = 0$  and  $\lambda^{(yx)1/2} > 0$ , then

$$\lim_{t \rightarrow \infty} z_i(t) = \frac{\lambda_i^{(yx)1/2}}{\lambda_i},$$

and the weight  $z_i(t)$  converges to the point  $z_i^* = \lambda_i^{(yx)1/2} / \lambda_i$  at a rate  $\mathcal{O}\left(e^{-\sqrt{\gamma^2 \lambda_i^2 + 4\eta^2 \lambda_i^{(yx)}} t}\right)$ .

We refer to appendix A.3, for the proof of proposition 1. We observe that the convergence rate is dependent on both of the singular values  $\lambda_i, \lambda_i^{(yx)1/2}$ , where the parameters  $\gamma, \eta$  control their respective influence. For a large absolute value of the conservation quantity  $\gamma$  (also referred to as the level of initialisation imbalance, see e.g. [22]), relative to the parameter  $\eta$ , the singular value  $\lambda_i$  of the input covariance matrix will dominate the rate of convergence. If instead the learning rate parameter  $\eta$  is large, relative to  $|\gamma|$ , the singular value  $\lambda_i^{(yx)1/2}$  of the input-output covariance matrix will dominate this rate.

Throughout the paper, we will pay special attention to two special cases of the dynamics. The first special case is  $\eta_a = 0$  ( $\eta = 0$ ), corresponding to the dynamics of the one-layer model, see e.g. [10], with solution

$$z_i(t) = e^{-|\gamma| \lambda_i t} (z_i(0) - \lambda_i^{(yx)1/2} \lambda_i^{-1}) + \lambda_i^{(yx)1/2} \lambda_i^{-1}, \quad (7)$$

with  $|cdot|$  an absolute value. The second special case is  $\gamma = 0$ , for which we recover the *balanced* dynamics, studied in e.g. [20, 10], with solution

$$z_i(t) = \frac{\lambda_i^{(yx)1/2} e^{2\eta \lambda_i^{(yx)1/2} t} z_i(0)}{\lambda (e^{2\eta \lambda_i^{(yx)1/2} t} - 1) z_i(0) + \lambda_i^{(yx)1/2}}. \quad (8)$$

We observe that these two special cases represents boundary cases of the general solution, in the sense that for  $\eta = 0$ , the time-dependent exponential term depends only on the singular value  $\lambda_i$ , and not on  $\lambda_i^{(yx)1/2}$ , while for  $\gamma = 0$ , the time dependent exponential term instead depends only on  $\lambda_i^{(yx)1/2}$ , and not on  $\lambda_i$ .

We note that under eq. (6), weights  $z_i(t)$  that are initialised at 0, by initialising  $a_i(0) = b_i(0) = 0$  (resulting in  $\gamma = 0$ ), will remain at 0. Hence, depending on the initialisation, only a subset of the diagonal elements of  $Z(t)$  will change during the course of learning. We will refer to these non-constant weights as *active* and use  $S_{\mathcal{A}} \subseteq \{1, 2, \dots, \min(d, d_y)\}$  with size  $|S_{\mathcal{A}}|$  to denote the set of indices corresponding to active weights in  $Z(t)$ .

### 3.2 Epoch-wise double descent in the two-layer model

We study the generalisation dynamics of  $Z$ , when weights are learned following the decoupled dynamics in eq. (6). First, for deriving the test MSE, we will assume that  $x$  is Gaussian with mean zero and true covariance matrix  $\bar{\Sigma}$ , written as  $x \sim \mathcal{N}(\mathbf{0}, \bar{\Sigma})$ . In addition, we assume that  $y$  follows a linear model

$$y = x\bar{W}^\top + \epsilon, \quad (9)$$

with true weights  $\bar{W} \in \mathbb{R}^{d_y \times d}$  and noise parameter  $\epsilon \sim \mathcal{N}(\mathbf{0}, \sigma^2 \mathbf{I}_{d_y})$ , where  $\mathbf{I}_{d_y}$  is the identity matrix of dimension  $d_y$ . Observe that in the synaptic weight space, the true weights are

$$\bar{Z} := U^{(yx)\top} \bar{W} V.$$

For the purpose of studying epoch-wise double descent, we derive a time-dependent expression for the generalisation error of the decoupled two-layer linear network. We note that similar derivations have been made previously. For example, [17] derive the test error for a two-layer linear neural network in a student-teacher setup, and under the assumptions  $\lambda_i = 1$  and  $\gamma = 0$ . Other examples include studies of the generalisation error of two-layer linear networks in online learning, see e.g. [12], or the derivation of the asymptotic generalisation error ( $t \rightarrow \infty$ ), see e.g. [13]. However, to the best of our knowledge, these studies deriving a time-dependent generalisation error for the two-layer model, have not made connections to the epoch-wise double descent phenomenon. We also note that the general expression for the generalisation error provided here, without making assumptions of the dynamics of  $z_i(t)$ , will naturally have similarities with corresponding expressions derived for the one-layer model, see e.g. [2, 15, 7].

**Proposition 2** *Consider the weight matrix  $Z(t)$  with weights  $z_i(t)$  following the decoupled dynamics in eq. (6). Assuming  $x \sim \mathcal{N}(\mathbf{0}, \bar{\Sigma})$  and that  $y$  follows the linear model given by eq. (9), the total generalisation error, using MSE as the error metric, can be decomposed as*

$$\begin{aligned} \mathcal{L}_{\mathcal{G}}(Z(t)) &= \mathbb{E}_x \left[ (\mathbf{y} - xW^\top)(\mathbf{y} - xW^\top)^\top \right] \\ &\approx \sum_{i \in S_{\mathcal{A}}} \lambda_i (\bar{z}_i - z_i(t))^2 + \text{const.}, \end{aligned} \quad (10)$$

with

$$\bar{z}_i = \lambda_i^{(yx)^{1/2}} \lambda_i^{-1} - \tilde{\epsilon}_i \lambda_i^{-1/2}.$$

We use the approximation  $\bar{\Sigma} \approx V \Sigma V^\top$  and let  $\tilde{\epsilon}_i$  denote the  $i^{\text{th}}$  element on the main diagonal of  $\tilde{\epsilon} := U^{(yx)\top} \epsilon U$ , with  $\epsilon = [\epsilon_1, \dots, \epsilon_n]^\top$ . The generalisation error is then a sum over individual error curves, being either monotonically decreasing,  $U$ -shaped, or monotonically increasing.

Following proposition 2, the total generalisation error of  $Z(t)$  is described by  $|S_{\mathcal{A}}|$  overlapping error curves. Note that, depending on the initialisation, and since  $Z(t)$  will remain diagonal in the decoupled dynamics, the test MSE might include additional constant terms, corresponding to diagonal elements  $z_i(t), i \notin S_{\mathcal{A}}$ , as well as non-diagonal elements of  $Z(t)$ . Moreover, for the approximation  $\bar{\Sigma} \approx V\Sigma V^\top$ , observe that  $\mathbb{E}_{\mathbf{X}}[V\Sigma V^\top] = \mathbb{E}_{\mathbf{X}}[n^{-1}\mathbf{X}^\top\mathbf{X}] = \bar{\Sigma}$ . Hence, we expect this approximation to become more accurate as  $n$  grows. We refer to appendix A.4, for the proof of proposition 2.

For the individual error curves in the sum of eq. (10) with each weight  $z_i(t)$  following the decoupled two-layer dynamics, eq. (6), we show that a single curve will never, by itself, exhibit a double descent pattern. Hence, similar to what has been observed for the one-layer model, see e.g. [15, 19], as well as the two-layer neural network with ReLU activation [15], epoch-wise double descent in the two-layer decoupled linear model, is a result of overlapping error curves, each corresponding to a single weight  $z_i(t)$ . To understand which factors give rise to the double descent behaviour, we therefore start by analysing these individual error curves.

First, observe that the initialisation  $z_i(0)$  as well as the position of the true minimum  $\bar{z}_i$  relative to  $z_i(0)$  and the global minimum  $z_i^*$ , will determine the behaviour of  $z_i(t)$ , as well as the shape of its error curve. For example, if  $z_i(0) > \lambda_i^{(yx)1/2}/\lambda$ ,  $z_i(t)$  will decrease in  $t$ , while for the opposite ( $z_i(0) < \lambda_i^{(yx)1/2}/\lambda$ ),  $z_i(t)$  will increase in  $t$ . Moreover, if  $\bar{z}_i$  does not lie on the path between the initialisation  $z_i(0)$  and the global minimum  $z_i^*$ , then  $z_i(t)$  will never pass this point and so, the corresponding error curve will be either monotonically decreasing or monotonically increasing in  $t$ . To limit the number of possible scenarios, we will restrict our analysis to the case where  $z_i(t)$  is positive and increasing in  $t$ . In addition, we will assume that  $\bar{z}_i \in [0, z_i^*]$ , noting that this also covers cases where the error curve of  $z_i(t)$  is monotonically increasing/decreasing in  $t$ , albeit with a focus on what we presume to be the most interesting scenario; the one where  $\bar{z}_i \in [z(0), z_i^*]$ , such that the error curve for  $z_i(t)$  is U-shaped. Hence, for our further analysis, we will make the following assumptions:

- (i) The model weight  $z_i(t)$  is initialised with  $\bar{z}_i \geq z_i(0) \geq 0$ , where  $z_i(0) = 0$  only if  $\gamma \neq 0$  and  $z_i(0) = \bar{z}_i$  only if  $\bar{z}_i < z_i^*$ .
- (ii) The  $i^{\text{th}}$  singular value of  $n^{-1}\mathbf{y}^\top\mathbf{X}$  is non-zero, i.e.  $\lambda_i^{(yx)1/2} > 0$ .
- (iii) If  $\eta = 0$ , the learning rates  $\eta_a, \eta_b$  and the initialisation of  $z_i(t)$  are chosen such that  $\gamma \neq 0$ . Similarly, if  $\gamma = 0$ , then the learning rates  $\eta_a, \eta_b$  are chosen such that  $\eta > 0$ .
- (iv) The minimum  $\bar{z}_i$  lies in the interval  $[0, z_i^*]$ , such that we can reparameterise  $\bar{z}_i = (1 - \rho_i)z_i^*$  with constant  $1 \geq \rho_i \geq 0$ .

Assumptions (i)-(iii) ensure that each  $z_i(t)$  is increasing in  $t$  and remains positive throughout training. Except for initialising  $z_i(t) \leq 0$ , we put an upper bound



$\bar{z}_i \geq z_i(0)$ , such that the weight  $z_i(t)$  is initialised before or at the true minimum,  $\bar{z}_i$ . Moreover, we exclude the cases  $z_i(0) = 0$  when  $\gamma = 0$  and  $z_i(0) = z_i^*$ , as they both lead to a constant  $z_i(t)$ , i.e.  $z_i(t)$  will not be active. For the same reason, we exclude the case  $\lambda_i^{(yx)1/2} = 0$ . Observe that as  $\text{rank}(\mathbf{y}^\top \mathbf{X}) \leq \text{rank}(\mathbf{X}^\top \mathbf{X})$ ,  $\lambda_i^{(yx)1/2} > 0$  implies  $\lambda_i > 0$ . Assumption (iii) ensures that the *effective* learning rate  $\sqrt{\gamma^2 + 4\eta z^2}$  is non-zero. Finally, assumption (iii) restricts  $\bar{z}_i$  to lie on the path between 0 and  $z_i^*$ . With this restriction, we put a focus on the scenarios where the error curve for  $z_i(t)$  is U-shaped, while still including scenarios where the error curve is monotonically decreasing in  $t$  ( $\rho_i = 0$ ) as well as monotonically increasing in  $t$  ( $1 \geq \rho_i \geq 1 - z(0)/z_i^*$ ). We emphasise that the purpose of assumptions (i)-(iv) is to limit the number of possible scenarios to be considered in our analysis of epoch-wise double descent, and that the analysis that follows could potentially be extended beyond assumptions (i)-(iv).

Observe that, with the reparametrisation of  $\bar{z}_i$  in terms of the parameter  $\rho_i$ , we can rewrite a single error term in the sum of eq. (10) as

$$\mathcal{L}_{\mathcal{G}}(z_i(t)) = \left( (1 - \rho_i) \lambda_i^{(yx)1/2} - \lambda_i z_i(t) \right)^2, \quad (11)$$

where the parameter  $\rho_i$  now determines the relative position of  $\bar{z}_i$  to the initialisation  $z_i(0)$  as well as the global minimum  $z_i^*$ , and hence the form of the generalisation curve. In special focus, will be the time it takes for  $z_i(t)$  to reach the true minimum  $\bar{z}_i$ , starting at  $z_i(0)$ , from now on denoted  $t_i^{(1-\rho_i)z_i^*}$ . Under assumptions (i)-(iv),  $t_i^{(1-\rho_i)z_i^*}$  is

$$t_i^{(1-\rho_i)z_i^*} = \frac{\log \left( \frac{\sqrt{\left( \gamma^2 \lambda_i^2 + 4\eta^2 \lambda_i^{(yx)} \right) \left( \gamma^2 \lambda_i^2 + 4\eta^2 \lambda_i^{(yx)} (1-\rho_i)^2 \right) + \gamma^2 \lambda_i^2 + 4\eta^2 \lambda_i^{(yx)} (1-\rho_i)}}{C \lambda_i^2 \lambda_i^{(yx)1/2} \rho_i} \right)}{\sqrt{\gamma^2 \lambda_i^2 + 4\eta^2 \lambda_i^{(yx)}}}, \quad (12)$$

with the constant  $C$  defined in proposition 1. See appendix A.3 for the derivation.

Starting from eq. (11), we provide the following two lemmas characterising the behaviour of the error curve  $\mathcal{L}_{\mathcal{G}}(z_i(t))$ .

**Lemma 1** *Consider the weight  $z_i(t)$  following the dynamics in eq. (6), under assumptions (i)-(iv). If  $1 \geq \rho_i > 0$ , the generalisation curve of  $z_i(t)$ , eq. (11), is convex at  $\bar{z}_i$ . If instead  $\rho_i = 0$ , the curve is convex leading up to the point  $\bar{z}_i$ , while  $\bar{z}_i$  itself is an undulation point.*

**Lemma 2** *Consider the weight  $z_i(t)$  following the dynamics in eq. (6). Under assumptions (i)-(iv), the generalisation curve for  $z_i(t)$ , eq. (11), has a maximum of three inflection points on the interval  $[0, \infty)$ , whereof a maximum of two lies in the interval  $(0, t_i^{(1-\rho_i)z_i^*})$ . Moreover, in the case that three inflection points*

exist and if  $5/7 > \rho_i > 0$ , then exactly two inflection points lie in the interval  $(0, t_i^{(1-\rho_i)z_i^*})$  and one in the interval  $(t_i^{(1-\rho_i)z_i^*}, \infty)$ .

We leave the proof of lemmas 1 and 2 to appendices A.5 and A.6. We highlight the following special cases of lemma 2:

- **One-layer dynamics ( $\eta = 0$ ).** For  $1 \geq \rho_i > 0$ , the error curve has one inflection point

$$\hat{t}_i^+ = \frac{\log\left(\frac{2(\lambda_i^{(yx)1/2} - \lambda_i z_i(0))}{\lambda_i^{(yx)1/2} \rho_i}\right)}{|\gamma| \lambda_i} \quad (13)$$

lying in the interval  $(t_i^{(1-\rho_i)z_i^*}, \infty)$ . For  $\rho_i = 0$ , the curve has no inflection points.

- **Balanced two-layer dynamics ( $\gamma = 0$ ).** For  $1 > \rho_i > 0$ , the error curve has up to two inflection points

$$\hat{t}_i^\pm = \frac{\log\left(\frac{(\lambda_i^{(yx)1/2} - \lambda_i z_i(0))(1 \pm \sqrt{\rho_i^2 - \rho_i + 1})}{\lambda_i \rho_i z_i(0)}\right)}{2\eta \lambda_i^{(yx)1/2}}, \quad (14)$$

one, if it exists, lying in the interval  $(0, t_i^{(1-\rho_i)z_i^*})$  and one in the interval  $(t_i^{(1-\rho_i)z_i^*}, \infty)$ . If  $\rho_i = 0$ , the curve has one potential inflection point

$$\hat{t}_i^- = \frac{\log\left(\frac{\lambda_i^{(yx)1/2} - \lambda_i z_i(0)}{2\lambda_i z_i(0)}\right)}{2\eta \lambda_i^{(yx)1/2}},$$

if it exists, lying in the interval  $(0, t_i^{(1-\rho_i)z_i^*})$ . In other words, for the balanced dynamics, the curve has up to two inflection points for  $1 > \rho_i > 0$ , lying on either side of  $t_i^{(1-\rho_i)z_i^*}$ , but only one inflection point if  $\rho_i = 0$ . For  $\hat{t}_i^-$  to exist, we require  $z_i(\hat{t}_i^-) \in (z_i(0), \bar{z}_i)$ .

Lemmas 1 and 2 tell us something about the general form of each individual error curve  $\mathcal{L}_{\mathcal{G}}(z_i(t))$ , eq. (11). We observe that under the one-layer model ( $\eta = 0$ ), the error curve  $\mathcal{L}_{\mathcal{G}}(z_i(t))$  has a maximum of one inflection point, with the curve being convex to start, and potentially becoming concave at a time point after  $t_i^{(1-\rho_i)z_i^*}$ . On the other hand, the error curve under the decoupled two-layer model can have up to three inflection points. With this, the error curve is potentially concave on parts of the time interval  $[0, t_i^{(1-\rho_i)z_i^*})$ . For the balanced dynamics, for example, the curve can, depending on the initialisation, be concave

to begin with, consistent with the initial plateau in learning previously observed for two-layer linear networks with small initialisation [2].

We will consistently use  $\hat{t}_i^-$  to denote the *maximum* inflection point of the error curve  $\mathcal{L}_G(z_i(t))$  located in the interval  $(0, t^{(1-\rho_i)z_i^*})$  and  $\hat{t}_i^+$  the *minimum* inflection point located in the interval  $(t^{(1-\rho_i)z_i^*}, \infty)$ . In other words, provided that they exist,  $\hat{t}_i^-$  and  $\hat{t}_i^+$  are the two inflection points located closest to, and on either side of, the minimum of  $\mathcal{L}_G(z_i(t))$ . Following lemma 1, the error curve is convex in between these points. We use this to find a necessary condition for epoch-wise double descent.

**Proposition 3** *Consider the weight matrix  $Z(t)$  with  $|S_A|$  active weights, following eq. (6). The total generalisation error, eq. (10), is a sum over  $|S_A|$  error curves. Under assumptions (i)-(iv), a necessary condition for this generalisation error to exhibit a double descent pattern over the course of learning, is that we can find at least one inflection point,  $\hat{t}$ , belonging to either one of the  $|S_A|$  individual error curves, such that*

$$\min\{t_i^{(1-\rho_i)z_i^*}; i \in S_A\} < \hat{t} < \max\{t_i^{(1-\rho_i)z_i^*}; i \in S_A\}.$$

Corollary 1 gives a necessary, but not sufficient, condition for epoch-wise double descent in the case of a general number of active weights  $|S_A|$ . We will study this condition further in the case of two active weights,  $z_i(t)$  and  $z_j(t)$ .

**Corollary 1** *Consider the weight matrix  $Z(t)$  with two active weights,  $z_i(t)$  and  $z_j(t)$ , following eq. (6) and for which, without loss of generality,  $t_i^{(1-\rho_i)z_i^*} < t_j^{(1-\rho_j)z_j^*}$ . The total generalisation error, eq. (10), is a sum over two error curves. Under assumptions (i)-(iv), a necessary condition for this generalisation error to exhibit a double descent pattern over the course of learning, is that we can find at least one inflection point,  $\hat{t}$ , belonging to either one of the two individual error curves, such that*

$$t_i^{(1-\rho_i)z_i^*} < \hat{t} < t_j^{(1-\rho_j)z_j^*}.$$

Moreover, provided that they exist, let  $\hat{t}_j^-$  denote the *maximum* inflection point of the error curve belonging to  $z_j(t)$ , and lying on the interval  $(0, t_j^{(1-\rho_j)z_j^*})$  and let  $\hat{t}_i^+$  denote the *minimum* inflection point belonging to the error curve of  $z_i(t)$  and lying on the interval  $(t_i^{(1-\rho_i)z_i^*}, \infty)$ . The necessary condition for epoch-wise double descent simplifies to fulfilling one of the following two conditions

$$\begin{aligned} t_i^{(1-\rho_i)z_i^*} &< \hat{t}_j^-, \\ \hat{t}_i^+ &< t_j^{(1-\rho_j)z_j^*}. \end{aligned}$$

From corollary 1, we observe that when  $Z$  has two active weights,  $z_i(t)$  and  $z_j(t)$ , epoch-wise double descent can happen in one of two scenarios. From an intuitive perspective, we might interpret the first scenario,  $t_i^{(1-\rho_i)z_i^*} < \hat{t}_j^-$ , as one where learning of the first weight,  $z_i(t)$ , tapers off at a point where the generalisation error of the second weight,  $z_j(t)$ , is still improving. Perhaps particularly so in the case  $5/7 > \rho_i > 0$ , where the minimum inflection point  $\hat{t}_i^+$  is the only inflection point of  $\mathcal{L}_{\mathcal{G}}(z_i(t))$  located after  $t_i^{(1-\rho_i)z_i^*}$  (see lemma 1). Similarly, we might interpret the second scenario,  $\hat{t}_i^+ < t_j^{(1-\rho_j)z_j^*}$ , as one where learning of the second weight,  $z_j(t)$ , starts taking off first after the first weight,  $z_i(t)$ , shows signs of overfitting. We refer to appendix A.7 for the proofs of proposition 3 and corollary 1.

Interestingly, we find that, while the necessary condition for epoch-wise double descent under the balanced dynamics, and with two active weights, also includes two scenarios in which double descent can occur, we find that the same necessary condition under the one-layer model only includes one of the two scenarios:

- **One-layer dynamics ( $\eta = 0$ ).** For  $1 \geq \rho_i > 0$ , let  $\hat{t}_i$  be the inflection point of the error curve corresponding to the weight  $z_i(t)$ , given by eq. (13). Then, the necessary condition for epoch-wise double descent with two active weights, given in corollary 1, simplifies to

$$\hat{t}_i < t_j^{(1-\rho_j)z_j^*}.$$

For vanishing initialisation ( $z_i(0) = z_j(0) = 0$ ), this condition simplifies further

$$\log\left(\frac{2}{\rho_i}\right) \leq \frac{\lambda_i}{\lambda_j} \log\left(\frac{1}{\rho_j}\right).$$

Thereby, providing us with a necessary condition for epoch-wise double descent under the one-layer model, that depends on the eigenvalues  $\lambda_i, \lambda_j$  of the input covariance matrix, but not the singular values  $\lambda_i^{(yx)^{1/2}}, \lambda_j^{(yx)^{1/2}}$ . Note that for  $\rho_i = 0$ , and when  $\eta = 0$ , there is no inflection point  $\hat{t}$  fulfilling the necessary condition of corollary 1.

- **Balanced two-layer dynamics ( $\gamma = 0$ ).** In the special case  $\gamma = 0$ , corresponding to the dynamics of the balanced two-layer model, let  $\hat{t}_j^-, \hat{t}_i^+$  be the inflection points given by eq. (14), for the error curves corresponding to the weights  $z_j(t), z_i(t)$ , respectively. The necessary condition for epoch-wise double descent with two active weights, given in corollary 1, corresponds to fulfilling at least one of the following two conditions:

- (i) For  $1 > \rho_j \geq 0$

$$t_i^{(1-\rho_i)z_i^*} < \hat{t}_j^-,$$

(ii) For  $1 > \rho_i > 0$

$$\hat{t}_i^+ < t_j^{(1-\rho_j)z_j^*}.$$

Observe that the second condition is not fulfilled for  $\rho_i = 0$ .

First, we notice that epoch-wise double descent with two active weights, can not happen if  $\rho_i = 0$ , where the error curve belonging to  $z_i(t)$  is monotonically decreasing. This is also true in the general case, as for  $\rho_i = 0$ , we have  $t_i^{(1-\rho_i)z_i^*} = t_i^{z_i^*} \rightarrow \infty$ . Similarly, double descent can not occur if  $\rho_j = 1$ , where the error curve belonging to  $z_j(t)$  is monotonically increasing, as for  $\rho_j = 1$ , we have  $t_j^{(1-\rho_j)z_j^*} = t_j^0 = 0$ .

More importantly, and as mentioned previously, there is only one scenario where epoch-wise double descent can happen in the one-layer model; namely the scenario where learning of the first weight,  $z_i(t)$ , starts to taper off at a point where the generalisation error of the second weight,  $z_j(t)$ , is still improving. Meanwhile, the necessary condition for epoch-wise double descent in the case  $\gamma = 0$ , i.e. the balanced dynamics, include the same two scenarios as in the general case, given by corollary 1, but where  $t_j^-, t_i^+$  are the only two inflection points that can lie in the interval  $(t_i^{(1-\rho_i)z_i^*}, t_j^{(1-\rho_j)z_j^*})$ .

Furthermore, for vanishing initialisation, we obtain a necessary condition for epoch-wise double descent in the one-layer model that is independent of the singular values of the input-output covariance matrix. This is in accordance with previous observations where only the eigenvalues  $\lambda_i, i \in S_{\mathcal{A}}$ , and not the singular values  $\lambda_i^{(yx)1/2}, i \in S_{\mathcal{A}}$ , have been identified as factors of epoch-wise double descent, attributing double descent to input features being learned at different speeds, see e.g. [15, 19, 7].

In simulations, see fig. 1, we also do not observe a relationship between epoch-wise double descent and the singular values  $\lambda_i^{(yx)1/2}, i \in S_{\mathcal{A}}$ , for the one-layer model, while we do observe such a dependence for the two-layer model (bottom row of fig. 1). Considering the balanced two-layer model,  $\gamma = 0$ , our findings are in accordance with observations made by e.g. [10], where the singular values  $\lambda_i^{(yx)1/2}, i \in S_{\mathcal{A}}$ , determines the learning speed at vanishing initialisation, although never coupled to the epoch-wise double descent phenomenon. Moreover, the findings align with proposition 1, where the singular values of the input-output covariance matrix have an effect on the convergence rate of the weight  $z_i(t)$  only when  $\eta > 0$ . Although, here we do find that also  $\lambda_i$  can be a factor of epoch-wise double descent in the case  $\gamma = 0$ , which is not indicated by this convergence rate.

In practice, we find that for very big differences in singular values (either  $\lambda_i$  or  $\lambda_i^{(yx)1/2}$ ), one error curve tends to dominate the sum of eq. (10), and thereby the double descent pattern is concealed. For the simulations in fig. 1, we therefore

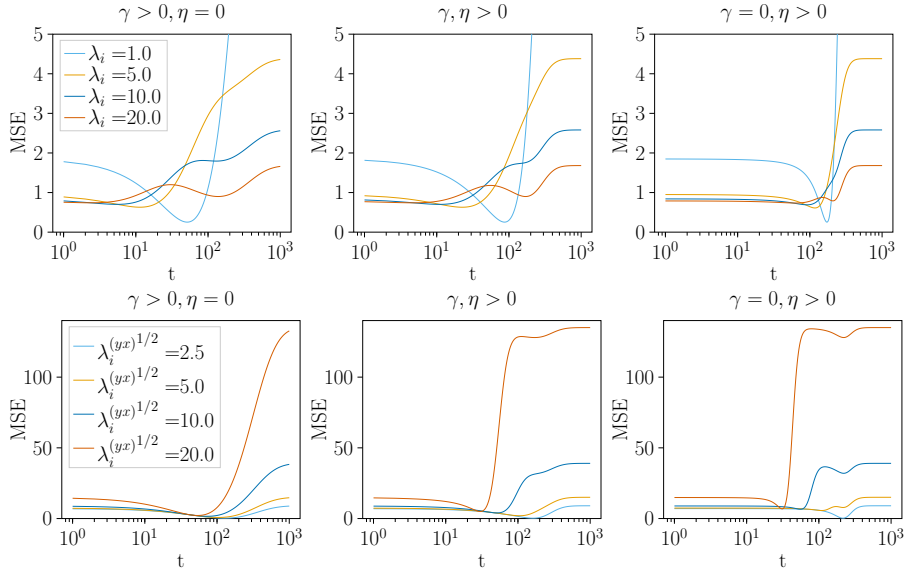


Figure 1: Examples of double descent with  $|S_{\mathcal{A}}| = 10$ , in three scenarios with different values of the parameters  $\gamma, \eta$ , and with two sets of active weights, one set evolving as  $z_i(t)$  and the other as  $z_j(t)$ . As default, parameters are set according to  $\lambda_i = \lambda_j = 1.0, \lambda_i^{(yx)1/2} = \lambda_j^{(yx)1/2} = 2.5, \rho_i = 0.5, \rho_j = 0.8$  and  $z_i(0) = z_j(0) = 0.01$ . **Top:** Changing  $\lambda_i$ . The weight  $z_i(t)$  has multiplicity 9, while  $z_j(t)$  has multiplicity 1. We observe double descent for large  $\lambda_i$  in all three scenarios, but double descent seems to appear for a smaller  $\lambda_i$  when  $\gamma$  is larger. **Bottom:** Changing  $\lambda_i^{(yx)1/2}$ . The weight  $z_i(t)$  has multiplicity 1, while  $z_j(t)$  has multiplicity 9. We observe double descent for large  $\lambda_i^{(yx)1/2}$  only in the scenarios where  $\eta > 0$ .

mimic the scenario where several weights have small or large singular values, by duplicating one of the weights  $z_i(t), z_j(t)$ .

Apart from the singular values,  $\lambda_i, \lambda_i^{(yx)1/2}, i \in S_{\mathcal{A}}$ , another factor that could potentially cause double descent, are relative distances to the true weights  $\bar{z}_i, i \in S_{\mathcal{A}}$  in the different dimensions, depending on the parameter  $\rho_i$ . The true noise model will indeed have an effect on double descent also in the single-layer model, see e.g. [21]. Moreover, differences in initialisation and learning rates, could also be factors affecting the form of the generalisation curve in eq. (10), including the potential emergence of a double descent pattern.

## 4 Discussion

We investigate epoch-wise double descent in decoupled two-layer linear networks, identifying factors of epoch-wise double descent in gradient-based learning. First, apart from differences in the eigenvalues of the input covariance matrix of the training data, also differences in the singular values of the input-output covariance matrix can cause epoch-wise double descent in the two-layer model. Second, by providing a necessary condition for epoch-wise double descent both for the standard linear regression model and for the linear decoupled two-layer network, we reveal an additional circumstance under which epoch-wise double descent can emerge in the two-layer model, not observed for the one-layer model.

There are several venues for further investigating epoch-wise double descent in (linear) neural networks, with the aim to better understand the causes of epoch-wise double descent in deep models. For one, it remains to be investigated if patterns in the training loss, such as the previously observed incremental learning pattern, see e.g. [10, 11, 5], could be indicators of epoch-wise double descent. Moreover, several assumptions were made leading up to the dynamics in eq. (6) and relaxing these assumptions could render new insights into the epoch-wise double descent phenomenon. We shortly discuss two extensions, namely that of deep(er) linear neural networks, as well as that of studying the dynamics of eq. (4) without decoupling of the weights.

**Incremental learning and epoch-wise double descent** Integral to understanding learning dynamics is the training loss, eq. (1). Rewriting eq. (1) in terms of the synaptic weight  $Z(t)$ , we find

$$\mathcal{L}(Z(t)) = \sum_{i \in S_{\mathcal{A}}} \lambda_i (z^* - z_i(t))^2 + \text{const.}, \quad (15)$$

where the constant term includes the error of possible inactive weights  $z_i(t)$ ,  $i \notin S_{\mathcal{A}}$ , as well as the residual error of the global minimum. We refer to appendix A.8 for the derivation. Under assumptions (i)-(iv), each term in the sum of eq. (15) will monotonically decrease to zero and so the training loss will be monotonically decreasing.

Previous studies on two-layer linear neural networks have discovered an implicit bias of gradient descent, causing an incremental learning pattern where weights are learned sequentially and where the training loss typically exhibits plateaus of close to constant error, see e.g. [11, 10, 5]. For the one-layer model, we can show that the training loss, eq. (15), is convex, and so it will not follow such a pattern, see appendix A.8. However, for the two-layer model, it would be an interesting venue to investigate whether incremental learning, bearing similarities with the epoch-wise double descent phenomenon, could be an indicator of epoch-wise double descent.

**Deeper models** While both the standard linear regression model and the two-layer linear neural network are indeed linear models, we have seen that

they exhibit different learning behaviours. Hence, as the number of layers,  $L$ , grows, we might expect the dynamics to change further. Let us consider the linear neural network with  $L$  layers, where the weight matrix in the synaptic weight space can be described as

$$Z = U^{(yx)\top} W V = \prod_{\ell=1}^L Z^{(\ell)},$$

each layer  $\ell$  represented by the weight matrix  $Z^{(\ell)}$  and with its own number of hidden units. Similar to the two-layer model, we can decouple the weights of  $Z(t)$ , such that they evolve independently. Then, to obtain an approximate dynamics for the  $i^{\text{th}}$  diagonal element,  $z_i(t)$ , of  $Z(t)$ , we make a number of simplifications, including assuming  $L$  to be even and large as well as grouping the model layers into two groups of equal learning rates and initialisation. The approximate dynamics are

$$\frac{dz_i}{dt} \approx \frac{L}{2} |\gamma| z_i^2 (\lambda_i^{(yx)1/2} - \lambda_i z_i). \quad (16)$$

We refer to appendix A.9 for the derivation. The dynamics in eq. (16) is similar to the dynamics of multi-layer linear neural networks found in [20], but with a weight  $\gamma$  and  $\lambda_i$  possibly separated from 1. The parameter  $\gamma$  is a conservation quantity, similar to the parameter  $\gamma$  in eq. (6). In the approximate  $L$ -layer dynamics, this parameter has a direct influence on the size of the gradient. Meanwhile the counterpart of the learning rate parameter,  $\eta$ , in the two-layer dynamics, vanishes as  $L$  grows large, although the learning rates of the layers still have an implicit effect on the learning dynamics through  $\gamma$ .

We observe that the dynamics in eq. (16) are cubic in  $z_i(t)$ . However, under the simplified assumptions made here, together with assumptions (i)-(iv) and provided that  $\gamma \neq 0, z_i(0) \neq 0$ , the error curve  $\mathcal{L}_{\mathcal{G}}(z_i(t))$ , eq. (11), will be monotonically decreasing, U-shaped, or monotonically increasing in  $t$ , just as the corresponding error curve under the decoupled two-layer dynamics, see appendix A.9. Moreover, the error curve  $\mathcal{L}_{\mathcal{G}}(z_i(t))$  will have at most two inflection points, indicating a necessary condition for epoch-wise double descent similar to the one given by corollary 1. With more relaxed assumptions, the error curve for the multi-layer dynamics might show more complex behaviour, potentially with additional, unidentified factors causing epoch-wise double descent in deeper models.

**The effect of coupling** In the decoupled dynamics, eq. (6), the weights in both the first and second layer of the two-layer network are each connected only to a single set of singular values  $\lambda_i, \lambda_i^{(yx)1/2}$ . If dynamics are not decoupled, however, weights can be connected to several singular values of both the input and input-output covariance matrices, resulting in interaction between weights in the learning dynamics, see e.g. [20, 2]. We might expect such an interaction to give rise to new types of epoch-wise double descent behaviours. For example,



in [15] it is hypothesised that epoch-wise double descent in two-layer neural networks with ReLU activation emerges because the weights in the second layer are learnt faster than the first layer weights. This could indicate a trade-off between independent evolution of weights and evolution through interaction. While not observed for the decoupled two-layer dynamics, it remains to be investigated if such a behaviour could also be observed in the (coupled) linear two-layer neural network.

## References

- [1] Ben Adlam and Jeffrey Pennington. Understanding Double Descent Requires a Fine-Grained Bias-Variance Decomposition. In *Advances in Neural Information Processing Systems*, 2020.
- [2] Madhu S. Advani, Andrew M. Saxe, and Haim Sompolinsky. High-dimensional dynamics of generalization error in neural networks. *Neural Networks*, 132:428–446, 2020.
- [3] Pierre Baldi and Yves Chauvin. Temporal Evolution of Generalization during Learning in Linear Networks. *Neural Computation*, 3(4):589–603, 1991.
- [4] Mikhail Belkin, Daniel Hsu, Siyuan Ma, and Soumik Mandal. Reconciling modern machine-learning practice and the classical bias-variance tradeoff. *Proceedings of the National Academy of Sciences*, 116(32):15849–15854, 2019.
- [5] Raphaël Berthier. Incremental Learning in Diagonal Linear Networks. *Journal of Machine Learning Research*, 24:1–26, 2023.
- [6] Antoine Bodin and Nicolas Macris. Model, sample, and epoch-wise descents: exact solution of gradient flow in the random feature model. *Advances in Neural Information Processing Systems*, 2021.
- [7] Antoine Bodin and Nicolas Macris. Gradient flow in the gaussian covariate model: exact solution of learning curves and multiple descent structures. *arXiv preprint arXiv:2212.06757*, 2022.
- [8] Alicia Curth, Alan Jeffares, and Mihaela van der Schaar. A U-turn on Double Descent: Rethinking Parameter Counting in Statistical Learning. In *Advances in Neural Information Processing Systems*, 2023.
- [9] Stéphane D’Ascoli, Levent Sagun, and Giulio Biroli. Triple Descent and the Two Kinds of Overfitting: Where & Why do they Appear? *Advances in Neural Information Processing Systems*, 2020.
- [10] Gauthier Gidel, Francis Bach, and Simon Lacoste-Julien. Implicit Regularization of Discrete Gradient Dynamics in Linear Neural Networks. *Advances in Neural Information Processing Systems*, 32, 2019.
- [11] Daniel Gissin, Shai Shalev-Shwartz, and Amit Daniely. The implicit bias of depth: How incremental learning drives generalization. In *International Conference on Learning Representations*, 2020.
- [12] Sebastian Goldt, Madhu S Advani, Andrew M Saxe, Florent Krzakala, and Lenka Zdeborová. Generalisation dynamics of online learning in over-parameterised neural networks. *arXiv preprint arXiv:1901.09085*, 2019.

- [13] Sebastian Goldt, Madhu S. Advani, Andrew M. Saxe, Florent Krzakala, and Lenka Zdeborová. Dynamics of stochastic gradient descent for two-layer neural networks in the teacher-student setup. *Journal of Statistical Mechanics: Theory and Experiment*, 2020(12):124010, 2020.
- [14] Trevor Hastie, Andrea Montanari, Saharon Rosset, and Ryan J. Tibshirani. Surprises in High-Dimensional Ridgeless Least Squares Interpolation. *The Annals of Statistics*, 50(2):949–986, 2022.
- [15] Reinhard Heckel and Fatih Furkan Yilmaz. Early stopping in deep networks: double descent and how to eliminate it. In *International Conference on Learning Representations*, 2021.
- [16] Daniel Kunin, Allan Raventós, Clémentine Dominé, Feng Chen, David Klindt, Andrew Saxe, and Surya Ganguli. Get rich quick: exact solutions reveal how unbalanced initializations promote rapid feature learning. *arXiv preprint arXiv:2406.06158*, 2024.
- [17] Andrew K. Lampinen and Surya Ganguli. An analytic theory of generalization dynamics and transfer learning in deep linear networks. In *International Conference on Learning Representations*, pages 1–20, 2019.
- [18] Preetum Nakkiran, Gal Kaplun, Yamini Bansal, Tristan Yang, Boaz Barak, and Ilya Sutskever. Deep double descent: Where bigger models and more data hurt. *Journal of Statistical Mechanics: Theory and Experiment*, 2021:124003, 2021.
- [19] Mohammad Pezeshki, Amartya Mitra, Yoshua Bengio, and Guillaume Lajoie. Multi-scale Feature Learning Dynamics: Insights for Double Descent. In *International Conference on Machine Learning*, 2022.
- [20] Andrew M. Saxe, James L. McClelland, and Surya Ganguli. Exact solutions to the nonlinear dynamics of learning in deep linear neural networks. In *International Conference on Learning Representations*, 2014.
- [21] Cory Stephenson and Tyler Lee. When and how epochwise double descent happens. *arXiv preprint arXiv:2108.12006*, 2021.
- [22] Salma Tarmoun, Guilherme França, Benjamin Haeffele, and René Vidal. Understanding the Dynamics of Gradient Flow in Overparameterized Linear Models. In *International Conference on Machine Learning*, volume 139, pages 10153–10161, 2021.

# Supplementary material for *Towards understanding epoch-wise double descent in two-layer linear neural networks*

## A Theoretical derivations

We provide derivations of the decoupled two-layer linear neural network dynamics as well as proofs for the main results of the paper. In the following derivations, we will use  $A_{i,:}$  and  $A_{:,i}$  to denote the  $i^{\text{th}}$  row and column, respectively, of a matrix  $A$ .

### A.1 Decoupled dynamics for two-layer linear networks

To derive the decoupled dynamics eq. (5), we start from the MSE criterion in eq. (1). Using  $\mathbf{y}^\top \mathbf{X} = n^{-1} U^{(yx)} \Sigma^{(yx)1/2} V^{(yx)\top}$  and  $n^{-1} \mathbf{X}^\top \mathbf{X} = V \Sigma V^\top$ , we have the following derivatives

$$\begin{aligned} \frac{d\mathcal{L}}{dW} &= \frac{1}{n} (\mathbf{y}^\top \mathbf{X} - W \mathbf{X}^\top \mathbf{X}) = (U^{(yx)} \Sigma^{(yx)1/2} V^{(yx)\top} - W V \Sigma V^\top), \\ \frac{d\mathcal{L}}{dW^{(1)}} &= W^{(2)\top} \frac{d\mathcal{L}}{dW}, \\ \frac{d\mathcal{L}}{dW^{(2)}} &= \frac{d\mathcal{L}}{dW} W^{(1)\top}, \end{aligned}$$

yielding the dynamics

$$\begin{aligned} \frac{1}{\eta_a} \frac{d}{dt} W^{(1)} &= W^{(2)\top} (U^{(yx)} \Sigma^{(yx)1/2} V^{(yx)\top} - W V \Sigma V^\top), \\ \frac{1}{\eta_b} \frac{d}{dt} W^{(2)} &= (U^{(yx)} \Sigma^{(yx)1/2} V^{(yx)\top} - W V \Sigma V^\top) W^{(1)\top}, \end{aligned}$$

with learning rates  $\eta_a, \eta_b \geq 0$ .

Following [20], we introduce the synaptic weights  $Z := Z^{(2)} Z^{(1)}$  with  $Z^{(1)} := W^{(1)} V^{(yx)\top}$ ,  $Z^{(2)} := U^{(yx)\top} W^{(2)}$ . The dynamics for  $Z^{(1)}$  are

$$\begin{aligned} \frac{1}{\eta_a} \frac{d}{dt} Z^{(1)} &= \frac{1}{\eta_a} \frac{d}{dt} W^{(1)} V^{(yx)} \\ &= W^{(2)\top} (U^{(yx)} \Sigma^{(yx)1/2} V^{(yx)\top} - W V \Sigma V^\top) V^{(yx)} \\ &= W^{(2)\top} (U^{(yx)} \Sigma^{(yx)1/2} - U^{(yx)} Z V^{(yx)\top} V \Sigma V^\top V^{(yx)}) \\ &= Z^{(2)\top} (\Sigma^{(yx)1/2} - Z V^{(yx)\top} V \Sigma V^\top V^{(yx)}). \end{aligned}$$

Similarly, the dynamics for  $Z^{(2)}$  are

$$\begin{aligned}\frac{1}{\eta_b} \frac{d}{dt} Z^{(2)} &= \frac{1}{\eta_b} U^{(yx)\top} \frac{d}{dt} W^{(2)} \\ &= U^{(yx)\top} (U^{(yx)} \Sigma^{(yx)1/2} V^{(yx)\top} - W V \Sigma V^\top) W^{(1)\top} \\ &= (\Sigma^{(yx)1/2} - Z V^{(yx)\top} V \Sigma V^\top V^{(yx)}) Z^{(1)\top}.\end{aligned}$$

Let  $V = [V_{:, \nu_1}^{(yx)}, V_{:, \nu_2}^{(yx)}, \dots, V_{:, \nu_d}^{(yx)}]$  for indices  $\nu_1, \nu_2, \dots, \nu_d \in \{1, 2, \dots, d\}$ ,  $\nu_i \neq \nu_j$  for  $i \neq j$ . In other words,  $V$  is equal to  $V^{(yx)}$  but with permuted columns. Then, the  $(i, j)$ <sup>th</sup> element of  $V^\top V^{(yx)}$  is

$$(V^\top V^{(yx)})_{i,j} = V_{:, \nu_i}^{(yx)} \cdot V_{:, j}^{(yx)} = \begin{cases} 1, & \text{if } \nu_i = j, \\ 0, & \text{otherwise,} \end{cases}$$

with  $\cdot$  the dot product.

Hence, the dynamics simplifies to

$$\begin{aligned}\frac{1}{\eta_a} \frac{d}{dt} Z^{(1)} &= Z^{(2)\top} (\Sigma^{(yx)1/2} - Z \tilde{\Sigma}), \\ \frac{1}{\eta_b} \frac{d}{dt} Z^{(2)} &= (\Sigma^{(yx)1/2} - Z \tilde{\Sigma}) Z^{(1)\top},\end{aligned}$$

where  $\tilde{\Sigma}$  is  $\Sigma$  but with diagonal elements reshuffled, such that  $\tilde{\Sigma}_{i,i} = \Sigma_{\nu_i, \nu_i}$ .

Now, let  $\alpha^{(i)}$  denote the  $i$ <sup>th</sup> column of  $Z^{(1)}$  and  $\beta^{(i)\top}$  denote the  $i$ <sup>th</sup> row of  $Z^{(2)}$ . Moreover, let  $\tilde{\lambda}_i$  and  $\lambda_i^{(yx)}$  be the  $i$ <sup>th</sup> diagonal elements of  $\tilde{\Sigma}$  and  $\Sigma^{(yx)}$ , respectively. We derive the dynamics for  $\alpha^{(i)}$ ,  $i = 1, \dots, d$ , and  $\beta^{(i)}$ ,  $i = 1, \dots, d_y$ .

We note that  $Z$  has elements

$$Z_{i,j} = \alpha^{(j)} \cdot \beta^{(i)},$$

and therefore

$$(Z \Sigma)_{i,j} = (\alpha^{(j)} \cdot \beta^{(i)}) \tilde{\lambda}_j.$$

Let  $S := \Sigma^{(yx)1/2} - Z \Sigma$ , with

$$S_{i,j} = \begin{cases} \lambda_i^{(yx)1/2} - (\alpha^{(i)} \cdot \beta^{(i)}) \tilde{\lambda}_i, & \text{if } j = i, \\ -(\alpha^{(j)} \cdot \beta^{(i)}) \tilde{\lambda}_j, & \text{otherwise.} \end{cases}$$

Then, for column  $\alpha^{(i)}$ ,

$$(Z^{(2)\top} S)_{i,j} = \sum_k \beta_i^{(k)} S_{k,j},$$

and, hence,

$$\frac{1}{\eta_a} \frac{d}{dt} \alpha^{(i)} = \sum_j \beta^{(j)} S_{j,i} = (\lambda_i^{(yx)1/2} - \tilde{\lambda}_i(\alpha^{(i)} \cdot \beta^{(i)})) \beta^{(i)} - \tilde{\lambda}_i \sum_{j \neq i} (\alpha^{(i)} \cdot \beta^{(j)}) \beta^{(j)}.$$

For row  $\beta^{(i)}$ , note

$$(SZ^{(1)\top})_{i,j} = \sum_k S_{i,k} \alpha_j^{(k)}.$$

Therefore,

$$\frac{1}{\eta_b} \frac{d}{dt} \beta^{(i)} = \sum_j S_{i,j} \alpha^{(j)} = (\lambda_i^{(yx)1/2} - \tilde{\lambda}_i(\alpha^{(i)} \cdot \beta^{(i)})) \alpha^{(i)} - \sum_{j \neq i} \tilde{\lambda}_j(\alpha^{(j)} \cdot \beta^{(i)}) \alpha^{(j)}$$

If we decouple modes by initialising  $\alpha^{(i)}, \beta^{(i)} \propto r^{(i)}$ , with  $r^{(i)}$  constant, orthogonal unit vectors, where  $r^{(i)} \cdot r^{(j)} = 0$  if  $i \neq j$ , we get

$$\begin{aligned} \frac{1}{\eta_a} \frac{d}{dt} \alpha^{(i)} &= (\lambda_i^{(yx)1/2} - \tilde{\lambda}_i(\alpha^{(i)} \cdot \beta^{(i)})) \beta^{(i)} \\ \frac{1}{\eta_b} \frac{d}{dt} \beta^{(i)} &= (\lambda_i^{(yx)1/2} - \tilde{\lambda}_i(\alpha^{(i)} \cdot \beta^{(i)})) \alpha^{(i)} \end{aligned}$$

We verify that, once decoupled, modes remain decoupled:

$$\begin{aligned} \frac{d}{dt}(\alpha^{(i)} \cdot \beta^{(j)}) &= \eta_a (\lambda_i^{(yx)1/2} - \tilde{\lambda}_i(\alpha^{(i)} \cdot \beta^{(i)})) \beta^{(i)} \cdot \beta^{(j)} \\ &\quad + \eta_b (\lambda_j^{(yx)1/2} - \tilde{\lambda}_j(\alpha^{(j)} \cdot \beta^{(j)})) \alpha^{(j)} \cdot \alpha^{(i)} \\ &= 0. \end{aligned}$$

We recover eq. (5), by rewriting the decoupled dynamics in terms of the scalar projections  $a_i = \alpha^{(i)} \cdot r^{(i)}$  and  $b_i = \beta^{(i)} \cdot r^{(i)}$

$$\begin{aligned} \frac{1}{\eta_a} \frac{da}{dt} &= \frac{1}{\eta_a} \frac{d}{dt} (\alpha^{(i)} \cdot r^{(i)}) = b_i (\lambda_i^{(yx)1/2} - \tilde{\lambda}_i a_i b_i), \\ \frac{1}{\eta_b} \frac{db}{dt} &= \frac{1}{\eta_b} \frac{d}{dt} (\beta^{(i)} \cdot r^{(i)}) = a_i (\lambda_i^{(yx)1/2} - \tilde{\lambda}_i a_i b_i). \end{aligned}$$

In addition, in the main paper, we assume  $V = V^{(yx)}$  such that  $\tilde{\Sigma} = \Sigma$ . Then, replace  $\tilde{\lambda}_i$  with  $\lambda_i$ , denoting the  $i^{\text{th}}$  diagonal element of  $\Sigma$ .

## A.2 Deriving the bridged dynamics

We derive the solution eq. (6), starting with deriving the bridged dynamics in eq. (6) from eq. (5). In the following, as we only consider a single weight, we will

drop all sub- and superscripts, *i*. Then, starting from eq. (6), let  $z = \alpha \cdot \beta = ab$ , for which

$$\frac{dz}{dt} = \frac{d}{dt}ab = (\eta_b a^2 + \eta_a b^2)(\lambda^{(yx)^{1/2}} - \lambda z).$$

We note that

$$\frac{d}{dt}(\eta_b a^2 - \eta_a b^2) = 2\eta_b a \frac{da}{dt} - 2\eta_a b \frac{db}{dt} = 0.$$

Hence,  $\eta_b a^2 - \eta_a b^2 = \gamma$  is constant. Therefore, we can rewrite

$$\frac{dz}{dt} = (\gamma + 2\eta_a b^2)(\lambda^{(yx)^{1/2}} - \lambda z)$$

From the equality

$$z = ab = \pm \sqrt{\frac{(\gamma + \eta_a b^2)}{\eta_b}} b,$$

we find

$$b = \pm \sqrt{\frac{-\gamma \pm \sqrt{\gamma^2 + 4\eta_a \eta_b z^2}}{2\eta_a}}.$$

Note that only the plus sign in the square root gives a valid solution for general  $\eta_a, \eta_b \geq 0, \gamma$ . Hence, we have

$$b^2 = \frac{-\gamma + \sqrt{\gamma^2 + 4\eta_a \eta_b z^2}}{2\eta_a}.$$

Replacing  $b^2$  in the current dynamics of  $z$  with this solution, we obtain

$$\frac{dz}{dt} = \sqrt{\gamma^2 + 4\eta^2 z^2}(\lambda^{(yx)^{1/2}} - \lambda z), \quad (17)$$

with  $\eta = \sqrt{\eta_a \eta_b}$ .

### A.3 Proof of proposition 1

For solving the differential equation, eq. (6), we focus on the case  $z(0) \leq \lambda^{(yx)^{1/2}}/\lambda$ . Note that eq. (6) is separable in  $z, t$ , and so

$$\int dt = \int \frac{dz}{\sqrt{\gamma^2 + 4\eta^2 z^2}(\lambda^{(yx)^{1/2}} - \lambda z)},$$

again dropping the subscript *i* for notational clarity. Assuming  $\lambda > 0$ , we solve the integrals to find

$$t = \frac{\log \left( \frac{\sqrt{(\gamma^2 \lambda^2 + 4\eta^2 \lambda^{(yx)})} (\gamma^2 + 4\eta^2 z^2) + \gamma^2 \lambda + 4\eta^2 \lambda^{(yx)^{1/2}} z}{\lambda(\lambda^{(yx)^{1/2}} - \lambda z)} \right)}{\sqrt{\gamma^2 \lambda^2 + 4\eta^2 \lambda^{(yx)}}} + C,$$

for a constant  $C$ . Now, solving for  $z = z(t)$ , with initial value  $z(0)$ , we obtain

$$z(t) = \frac{C^2 \lambda^2 \lambda^{(yx)^{1/2}} e^{2\sqrt{\gamma^2 \lambda^2 + 4\eta^2 \lambda^{(yx)}} t} - 2C\gamma^2 \lambda^2 e^{\sqrt{\gamma^2 \lambda^2 + 4\eta^2 \lambda^{(yx)}} t} - 4\gamma^2 \eta^2 \lambda^{(yx)^{1/2}}}{\lambda \left( C^2 \lambda^2 e^{2\sqrt{\gamma^2 \lambda^2 + 4\eta^2 \lambda^{(yx)}} t} + 8C\eta^2 \lambda^{(yx)^{1/2}} e^{\sqrt{\gamma^2 \lambda^2 + 4\eta^2 \lambda^{(yx)}} t} - 4\gamma^2 \eta^2 \right)},$$

with

$$C = \frac{\sqrt{(\gamma^2 \lambda^2 + 4\eta^2 \lambda^{(yx)}) (\gamma^2 + 4\eta^2 z(0)^2) + \gamma^2 \lambda + 4\eta^2 \lambda^{(yx)^{1/2}} z(0)}}{\lambda (\lambda^{(yx)^{1/2}} - \lambda z(0))},$$

which finishes the proof of the first part of proposition 1. Before moving on to the next part of the proof, we point out that we recover eqs. (7) and (8), by inserting  $\eta = 0$  and  $\gamma = 0$ , respectively, into the solution. Moreover, note that the solution to the dynamics, eq. (6), includes solving the equation

$$\begin{aligned} & \sqrt{(\gamma^2 \lambda^2 + 4\eta^2 \lambda^{(yx)}) (\gamma^2 + 4\eta^2 z(0)^2)} \\ &= \lambda (\lambda^{(yx)^{1/2}} - \lambda z(t)) C e^{\sqrt{\gamma^2 \lambda^2 + 4\eta^2 \lambda^{(yx)}} t} - \gamma^2 \lambda - 4\eta^2 \lambda^{(yx)^{1/2}} z(t), \end{aligned}$$

for which we require

$$\lambda (\lambda^{(yx)^{1/2}} - \lambda z(t)) C e^{\sqrt{\gamma^2 \lambda^2 + 4\eta^2 \lambda^{(yx)}} t} - \gamma^2 \lambda - 4\eta^2 \lambda^{(yx)^{1/2}} z(t) \geq 0.$$

To verify that this holds, we rewrite

$$\begin{aligned} & \lambda (\lambda^{(yx)^{1/2}} - \lambda z(t)) C e^{\sqrt{\gamma^2 \lambda^2 + 4\eta^2 \lambda^{(yx)}} t} - \gamma^2 \lambda - 4\eta^2 \lambda^{(yx)^{1/2}} z(0) \\ &= \frac{(\gamma^2 \lambda^2 + 4\eta^2 \lambda^{(yx)}) (C^2 \lambda^2 e^{2\sqrt{\gamma^2 \lambda^2 + 4\eta^2 \lambda^{(yx)}} t} + 4\gamma^2 \eta^2)}{\lambda (C^2 \lambda^2 e^{2\sqrt{\gamma^2 \lambda^2 + 4\eta^2 \lambda^{(yx)}} t} + 8C\eta^2 \lambda^{(yx)^{1/2}} e^{\sqrt{\gamma^2 \lambda^2 + 4\eta^2 \lambda^{(yx)}} t} - 4\gamma^2 \eta^2)}. \end{aligned}$$

We observe that the nominator is positive. For the denominator, note that for  $z(0) < \lambda^{(yx)^{1/2}}/\lambda$ , we have  $C \geq 0$  and therefore

$$\begin{aligned} & \lambda (C^2 \lambda^2 e^{2\sqrt{\gamma^2 \lambda^2 + 4\eta^2 \lambda^{(yx)}} t} + 8C\eta^2 \lambda^{(yx)^{1/2}} e^{\sqrt{\gamma^2 \lambda^2 + 4\eta^2 \lambda^{(yx)}} t} - 4\gamma^2 \eta^2) \\ & \geq \lambda (C^2 \lambda^2 + 8C\eta^2 \lambda^{(yx)^{1/2}} - 4\gamma^2 \eta^2). \end{aligned}$$

We find

$$\begin{aligned} & \lambda (C^2 \lambda^2 + 8C\eta^2 \lambda^{(yx)^{1/2}} - 4\gamma^2 \eta^2) \\ &= \frac{2(\gamma^2 \lambda^2 + 4\eta^2 \lambda^{(yx)})}{\lambda^2 (\lambda^{(yx)^{1/2}} - \lambda z(0))^2} \\ & \quad \cdot \left( \gamma^2 \lambda + 4\eta^2 \lambda^{(yx)^{1/2}} z(0) + \sqrt{(\gamma^2 \lambda^2 + 4\eta^2 \lambda^{(yx)}) (\gamma^2 + 4\eta^2 z(0)^2)} \right), \end{aligned}$$

which is positive for  $z(0) < \lambda^{(yx)^{1/2}}/\lambda$ , and so, the solution holds.



For the next part of proposition 1, we take the limit of the solution,  $z(t)$ , to find

$$\lim_{t \rightarrow \infty} z(t) = \begin{cases} \frac{\lambda^{(yx)1/2}}{\lambda}, & \text{if } \gamma \neq 0, \\ \frac{\lambda^{(yx)1/2}}{\lambda}, & \text{if } \gamma = 0, z(0) > 0, \\ 0, & \text{otherwise.} \end{cases}$$

In addition, observe that, for moderately large  $t$ , and assuming  $z(0) > 0$  in the special case  $\gamma = 0, \lambda^{(yx)1/2} > 0$ , we have

$$\begin{aligned} |z^* - z(t)| &= \left| \frac{2C e^{\sqrt{\gamma^2 \lambda^2 + 4\eta^2 \lambda^{(yx)} t} (\gamma^2 \lambda^2 + 4\eta^2 \lambda^{(yx)})}}{\lambda \left( C^2 \lambda^2 e^{2\sqrt{\gamma^2 \lambda^2 + 4\eta^2 \lambda^{(yx)} t} (\gamma^2 \lambda^2 + 4\eta^2 \lambda^{(yx)})} + 8C\eta^2 \lambda^{(yx)1/2} e^{\sqrt{\gamma^2 \lambda^2 + 4\eta^2 \lambda^{(yx)} t} (\gamma^2 \lambda^2 + 4\eta^2 \lambda^{(yx)})} - 4\gamma^2 \eta^2 \right)} \right| \\ &\simeq \left| 2C^{-1} \lambda^{-3} (\gamma^2 \lambda^2 + 4\eta^2 \lambda^{(yx)}) e^{-\sqrt{\gamma^2 \lambda^2 + 4\eta^2 \lambda^{(yx)} t}} \right|, \end{aligned}$$

with  $|\cdot|$  denoting an absolute value and with  $z^* = \lambda^{(yx)1/2}/\lambda$ .

#### A.4 Proof of proposition 2

For the first part of the proof of proposition 2, we derive eq. (10), starting from

$$\mathcal{L}_{\mathcal{G}}(W) = \frac{1}{2} \mathbb{E}_{x,y} \left[ (y - xW(t)^\top)(y - xW(t)^\top)^\top \right],$$

with  $x \sim \mathcal{N}(\mathbf{0}, \bar{\Sigma})$  and  $y$  defined in eq. (9).

First, we rewrite  $\bar{W} = U^{(yx)} \bar{Z} V^{(yx)\top}$  in eq. (9) in terms of the global minimum

$$\mathbf{y}^\top \mathbf{X} (\mathbf{X}^\top \mathbf{X})^\dagger = U^{(yx)} \Sigma^{(yx)} \Sigma^\dagger V^\top,$$

where  $\dagger$  denotes the Moore-Penrose pseudoinverse. Observe that the global minimum can also be expressed using eq. (9) according to

$$\begin{aligned} \mathbf{y}^\top \mathbf{X} (\mathbf{X}^\top \mathbf{X})^\dagger &= (\bar{W} \mathbf{X}^\top \mathbf{X} + \epsilon^\top \mathbf{X}) (\mathbf{X}^\top \mathbf{X})^\dagger \\ &= (\bar{W} V \Sigma + \epsilon^\top U \Sigma^{1/2}) \Sigma^\dagger V^\top, \end{aligned}$$

with  $\epsilon = [\epsilon_1, \dots, \epsilon_n]^\top$ , the matrix of residual vectors  $\epsilon_i = y_i - x_i \bar{W}^\top$ ,  $i = 1, \dots, n$ . Using the two equations for the global minimum, we find

$$\begin{aligned} \bar{W} &= U^{(yx)} (\Sigma^{(yx)1/2} - U^{(yx)\top} \epsilon^\top U (\Sigma^{1/2})^\dagger) V^\top \\ &= U^{(yx)} (\Sigma^{(yx)1/2} - \tilde{\epsilon}^\top (\Sigma^{1/2})^\dagger) V^\top, \end{aligned}$$

with  $\tilde{\epsilon} := U^{(yx)\top} \epsilon U$ . The true weights in the synaptic weight space are  $\bar{Z} := U^{(yx)\top} \bar{W} V = \Sigma^{(yx)1/2} - \tilde{\epsilon}^\top (\Sigma^{1/2})^\dagger$ .

Now, in the synaptic weight space, using  $x \sim \mathcal{N}(\mathbf{0}, \bar{\Sigma})$  and with  $y$  following eq. (9), we have

$$\begin{aligned}
\mathcal{L}_{\mathcal{G}}(Z(t)) &= \frac{1}{2} \mathbb{E}_{x,y} \left[ \left( y - x(U^{(yx)} Z(t) V^\top)^\top \right) \left( y - x(U^{(yx)} Z(t) V^\top)^\top \right)^\top \right] \\
&= \frac{1}{2} \mathbb{E}_{x,y} \left[ \left( xV(\bar{Z} - Z(t))^\top U^{(yx)\top} + \epsilon \right) \left( xV(\bar{Z} - Z(t))^\top U^{(yx)\top} + \epsilon \right)^\top \right] \\
&= \frac{1}{2} \mathbb{E}_{x,y} \left[ xV(\bar{Z} - Z(t))^\top (\bar{Z} - Z(t)) V^\top x^\top + \right. \\
&\quad \left. 2xV(\bar{Z} - Z(t))^\top U^{(yx)\top} \epsilon^\top + \epsilon \epsilon^\top \right] \\
&= \frac{1}{2} \left( \mathbb{E}_{x,y} \left[ xV(\bar{Z} - Z(t))^\top (\bar{Z} - Z(t)) V^\top x^\top \right] + \sigma^2 \mathbb{I} \right) \\
&\stackrel{(1)}{=} \frac{1}{2} \left( \text{Tr} \left( (\bar{Z} - Z(t))^\top (\bar{Z} - Z(t)) V^\top \bar{\Sigma} V \right) + \sigma^2 \mathbb{I} \right) \\
&\stackrel{(2)}{\approx} \frac{1}{2} \left( \text{Tr} \left( (\bar{Z} - Z(t))^\top (\bar{Z} - Z(t)) \Sigma \right) + \sigma^2 \mathbb{I} \right) \\
&= \frac{1}{2} \left( \text{Tr} \left( (\Sigma^{(yx)1/2} - \tilde{\epsilon}^\top (\Sigma^{1/2})^\dagger - Z(t))^\top \right. \right. \\
&\quad \left. \left. (\Sigma^{(yx)1/2} - \tilde{\epsilon}^\top (\Sigma^{1/2})^\dagger - Z(t)) \Sigma \right) + \sigma^2 \mathbb{I} \right) \\
&= \frac{1}{2} \sum_{i \in S_{\mathcal{A}}} \lambda_i (\lambda_i^{(yx)1/2} \lambda_i^{-1} - \tilde{\epsilon}_i \lambda_i^{-1/2} - z_i(t))^2 + \text{const.},
\end{aligned}$$

resulting in eq. (10) with  $\tilde{\epsilon}_i$  the  $i^{\text{th}}$  element on the main diagonal of  $\tilde{\epsilon}$ . In (1), we use  $\mathbb{E}_x[xAx^\top] = \text{Tr}(A\bar{\Sigma})$ , with  $A = V(\bar{Z} - Z(t))^\top (\bar{Z} - Z(t)) V^\top$ , together with the cyclic property of the trace, and in (2) we use the approximation  $V\Sigma V^\top \approx \bar{\Sigma}$ . The final constant term includes the noise term  $\sigma^2 \mathbb{I}$  as well as a possible constant error corresponding to constant entries in  $Z(t)$ , including non-diagonal elements for which corresponding entries in  $\bar{Z}$  are non-zero.

For the second part of the proof, consider an individual error curve in the sum of eq. (10), which has the form

$$\mathcal{L}_{\mathcal{G}}(z_i(t)) = \lambda_i (\lambda_i^{(yx)1/2} \lambda_i^{-1} - \tilde{\epsilon}_i \lambda_i^{-1/2} - z_i(t))^2.$$

To show that this error curve is either monotonically decreasing, U-shaped, or monotonically increasing in  $t$ , we study the gradient

$$\frac{d}{dt} \mathcal{L}_{\mathcal{G}}(z_i(t)) = -2\lambda_i (\lambda_i^{(yx)1/2} \lambda_i^{-1} - \tilde{\epsilon}_i \lambda_i^{-1/2} - z_i(t)) \frac{dz_i(t)}{dt}.$$

Following the dynamics in eq. (6), the sign of  $dz_i(t)/dt$  will be determined by the term  $(\lambda_i^{(yx)1/2} - \lambda z_i(t))$  and hence on the initialisation. If  $z_i(0) \leq z_i^*$ ,  $z_i(t)$  will monotonically increase in  $t$  with

$$\frac{dz_i(t)}{dt} \geq 0, \forall t.$$

On the other hand, if  $z_i(0) > z_i^*$ ,  $z_i(t)$  will monotonically decrease in  $t$  with

$$\frac{dz_i(t)}{dt} \leq 0, \forall t.$$

With this in mind, observe that the gradient of the error curve  $\mathcal{L}_{\mathcal{G}}(z_i(t))$  will change signs only at one point. We see this by solving

$$\frac{d}{dt}\mathcal{L}_{\mathcal{G}}(z_i(t)) = 0.$$

While one solution to this equation is  $dz_i(t)/dt = 0$ , we note that the gradient will not change signs at this point. Indeed if  $dz_i(t)/dt = 0$ ,  $z_i(t)$  will remain at its current value, and so will  $\mathcal{L}_{\mathcal{G}}(z_i(t))$ . The other solution is

$$z_i(t) = \lambda_i^{(yx)1/2} \lambda_i^{-1} - \tilde{\epsilon}_i \lambda_i^{-1/2},$$

and as  $z_i(t)$  is either monotonically increasing or decreasing in  $t$ , this point will be passed only once during the course of learning.

Now, following eq. (6),  $z_i(t)$  will either increase or decrease in  $t$ , depending on the initialisation, starting at  $z_i(0)$  and ending at  $z_i^*$ . An exception can be seen in the special case  $\gamma = 0$  and  $z_i(0) \leq 0$ , where the trajectory will stop at  $z_i(t) = 0$ . We observe that if

$$\lambda_i^{(yx)1/2} \lambda_i^{-1} - \tilde{\epsilon}_i \geq z_i^* \geq z_i(0),$$

or

$$z_i(0) > z_i^* \geq \lambda_i^{(yx)1/2} \lambda_i^{-1} - \tilde{\epsilon}_i \lambda_i^{-1/2},$$

then

$$\frac{d}{dt}\mathcal{L}_{\mathcal{G}}(z_i(t)) \leq \forall t,$$

and so the error curve is monotonically decreasing in  $t$ . If instead

$$z_i^* \geq z_i(0) \geq \lambda_i^{(yx)1/2} \lambda_i^{-1} - \tilde{\epsilon}_i,$$

or

$$\lambda_i^{(yx)1/2} \lambda_i^{-1} - \tilde{\epsilon}_i \lambda_i^{-1/2} \geq z_i(0) > z_i^*,$$

then,

$$\frac{d}{dt}\mathcal{L}_{\mathcal{G}}(z_i(t)) \geq \forall t,$$

and the error curve is monotonically increasing in  $t$ . Finally, if the point  $\lambda_i^{(yx)1/2} \lambda_i^{-1} - \tilde{\epsilon}_i \lambda_i^{-1/2}$  lies on the path between  $z_i(0)$  and the global minimum  $z_i^*$  (or alternatively, the fixed point  $z_i(t) = 0$  if  $\gamma = 0, z_i(t) \leq 0$ ), i.e. if

$$z_i^* > \lambda_i^{(yx)1/2} \lambda_i^{-1} - \tilde{\epsilon}_i > z_i(0),$$

or

$$z_i(0) > \lambda_i^{(yx)1/2} \lambda_i^{-1} - \tilde{\epsilon}_i > z_i^*,$$

the error curve  $\mathcal{L}_{\mathcal{G}}(z_i(t))$  will be decreasing in  $t$  up until the point  $z_i(t) = \lambda_i^{(yx)1/2} \lambda_i^{-1} - \tilde{\epsilon}_i \lambda_i^{-1/2}$ , after which the derivative of the error curve will change signs, and the error will become increasing in  $t$ . The resulting error curve hence will follow a U-shape. An exception can be seen for the case  $\gamma = 0$  and  $z(0) \leq 0$ , where the trajectory might stop before the point  $z_i(t) = \lambda_i^{(yx)1/2} \lambda_i^{-1} - \tilde{\epsilon}_i \lambda_i^{-1/2}$ . In this case, the error curve will yet again be monotonically decreasing in  $t$ .

To conclude, each error curve  $\mathcal{L}_{\mathcal{G}}(z_i(t))$  as part of the sum in eq. (10), will be either monotonically decreasing, U-shaped, or monotonically increasing in  $t$ , and so the full generalisation curve is a sum of monotonically decreasing, U-shaped, or monotonically increasing curves, finishing the proof of proposition 2.

## A.5 Proof of lemma 1

To prove lemma 1, we first note that, with  $z(t)$  following eq. (6), the second derivative of  $z(t)$  with respect to  $t$  is

$$\frac{d^2 z(t)}{dt^2} = 4\eta^2 z(t) (\lambda^{(yx)1/2} - \lambda z(t))^2 - \lambda (\gamma^2 + 4\eta^2 z(t)^2) (\lambda^{(yx)1/2} - \lambda z(t)),$$

dropping all subscripts  $i$  for notational clarity.

The first and second time derivatives of  $\mathcal{L}_{\mathcal{G}}(z(t))$  follow as

$$\begin{aligned} \frac{d}{dt} \mathcal{L}_{\mathcal{G}}(z(t)) &= -2\lambda(\bar{z} - z(t)) \frac{dz(t)}{dt} \\ &= -2\lambda(\bar{z} - z(t)) \sqrt{\gamma^2 \lambda^2 + 4\eta^2 \lambda^{(yx)}} (\lambda^{(yx)1/2} - \lambda z(t)), \quad (18) \\ \frac{d^2}{dt^2} \mathcal{L}_{\mathcal{G}}(z(t)) &= 2\lambda \left( \frac{dz(t)}{dt} \right)^2 - 2\lambda(\bar{z} - z(t)) \frac{d^2 z(t)}{dt^2} \\ &= 2\lambda (\lambda^{(yx)1/2} - \lambda z(t)) \left( (\gamma^2 + 4\eta^2 z(t)^2) (\lambda^{(yx)1/2} + \lambda \bar{z} - 2\lambda z(t)) \right. \\ &\quad \left. - 4\eta^2 z(t) (\bar{z} - z(t)) (\lambda^{(yx)1/2} - \lambda z(t)) \right). \quad (19) \end{aligned}$$

Then, the second derivative at  $z(t) = \bar{z}$  is

$$\left. \frac{d^2}{dt^2} \mathcal{L}_{\mathcal{G}}(z(t)) \right|_{z(t)=\bar{z}} = \frac{2\rho^2 \lambda^{(yx)} (\gamma^2 \lambda^2 + 4\eta^2 \lambda^{(yx)} (1 - \rho)^2)}{\lambda}, \quad (20)$$

replacing  $\bar{z} = (1 - \rho)\lambda^{(yx)1/2}/\lambda$ . We immediately see that this derivative is positive if  $1 \geq \rho > 0$ , with an exception for the case  $\rho = 1$  if  $\gamma = 0$ , but note that this scenario is not included under assumptions (i)-(iv).

For  $\rho = 0$ , to see that the curve is convex leading up to the point  $\bar{z}$ , note that solving

$$\frac{d^2}{dt^2}\mathcal{L}_{\mathcal{G}}(z(t)) = 0,$$

gives two potential inflection points

$$\hat{z}^{\pm} = \frac{\eta\lambda^{(yx)1/2} \pm \sqrt{\eta^2\lambda^{(yx)} - 6\gamma^2\lambda^2}}{6\lambda\eta}.$$

(the other solutions are undulation points). The roots  $\hat{z}^{\pm}$  are real if  $\eta^2\lambda^{(yx)} \geq 6\gamma^2\lambda^2$  (including the case  $\gamma = 0$ ). In this case, observe that we can upper bound the square root  $\sqrt{\eta^2\lambda^{(yx)} - 6\gamma^2\lambda^2} \leq \eta\lambda^{(yx)1/2}$ , and so

$$\hat{z}^{\pm} \leq \frac{\lambda^{(yx)1/2}}{3\lambda}.$$

Observe that this upper bound lies before the point  $\bar{z} = z^*$ . Evaluating the second curve at a point beyond the upper bound, we find

$$\left. \frac{d^2}{dt^2}\mathcal{L}_{\mathcal{G}}(z_i(t)) \right|_{z(t)=\frac{\lambda^{(yx)1/2}}{2\lambda}} = \gamma^2\lambda\lambda^{(yx)} + \frac{\eta^2\lambda^{(yx)2}}{2\lambda} > 0,$$

with the inequality following from assumptions (i)-(iv). Hence, the curve is convex leading up to the minimum  $\bar{z}$ . If instead  $\eta^2\lambda^{(yx)} < 6\gamma^2\lambda^2$  (including the case  $\eta = 0$ ), then the roots  $\hat{z}^{\pm}$  are complex, and so there are no inflection points in the error curve. As we have shown that the curve is convex at a point in the curve, the curve must be convex on the full path, and so, again, it must be convex leading up to the minimum. Since for  $\rho = 0$ , the true minimum  $\bar{z}$  is equal to the global minimum  $z^*$ , which is reached at  $t \rightarrow \infty$ , the error curve will gradually go towards 0 as  $t \rightarrow \infty$ . While the second derivative is 0 at  $\bar{z}$  if  $\rho = 0$ , see eq. (20), the error curve will not change convexity at this point, and hence, the minimum is an undulation point. This concludes the proof of lemma 1.

## A.6 Proof of lemma 2

For proving lemma 2, we seek the inflection points of the error curve eq. (11), with  $z(t)$  following eq. (6) and under assumptions (i)-(iv) introduced in the main paper. As in previous derivations, we will, for notational clarity, drop all subscripts  $i$ .

The first and second time derivatives of  $\mathcal{L}_{\mathcal{G}}(z(t))$  are given in eqs. (18) and (19). Before moving on to analysing the inflection points of the error curve,

we evaluate its second derivative at the point  $z(t) = 0$

$$\left. \frac{d^2}{dt^2} \mathcal{L}_G(z(t)) \right|_{z(t)=0} = 2\gamma^2 \lambda \lambda^{(yx)} (2 - \rho).$$

We observe that under assumptions (i)-(iv), the second derivative is positive (or zero) at  $z(t) = 0$ .

For analysing the inflection points, we solve

$$\frac{d^2}{dt^2} \mathcal{L}_G(z(t)) = 0,$$

with respect to  $z(t)$ , yielding

$$2(\lambda^{(yx)1/2} - \lambda z(t)) = 0,$$

or

$$\begin{aligned} & \lambda((\gamma^2 + 4\eta^2 z(t)^2)(\lambda^{(yx)1/2} + \lambda \bar{z} - 2\lambda z(t)) \\ & - 4\eta^2 z(t)(\bar{z} - z(t))(\lambda^{(yx)1/2} - \lambda z(t))) = 0. \end{aligned}$$

The solution to the first equation is  $z(t) = z^*$ . This is not an inflection point, but instead an undulation point, since  $z(t)$  will not grow beyond its global minimum, and hence, the curve will not change convexity at this point. We instead continue by analysing the second equation, amounting to analysing the roots of the polynomial

$$\begin{aligned} f(z(t)) &= a_z z(t)^3 + b_z z(t)^2 + c_z z(t) + d_z, \\ a_z &= 12\lambda^2 \eta^2, \\ b_z &= -8\eta^2 \lambda \lambda^{(yx)1/2} (2 - \rho), \\ c_z &= 2(\gamma^2 \lambda^2 + 2\eta^2 \lambda^{(yx)} (1 - \rho)), \\ d_z &= -\gamma^2 \lambda \lambda^{(yx)1/2} (2 - \rho). \end{aligned}$$

We observe that the polynomial  $f(z(t))$  with  $\gamma \neq 0, \eta > 0$  is cubic in  $z(t)$ , and has a maximum of three real roots, possibly corresponding to inflection points in the error curve  $\mathcal{L}_G(z(t))$ . As there are no other possible inflection points, the error curve  $\mathcal{L}_G(z(t))$  has a maximum of three inflection points on the interval  $[0, z^*]$ . This finishes the proof of the first part of lemma 2.

For analysing the relative positions of the potential inflection points of  $\mathcal{L}_G(z(t))$ , we will separate our further analysis into three cases: (i)  $\gamma \neq 0, \eta > 0$ , (ii)  $\gamma \neq 0, \eta = 0$ , (iii)  $\gamma = 0, \eta > 0$ .

**Case  $\gamma \neq 0, \eta > 0$ .** We start with the general case, assuming  $\gamma \neq 0, \eta > 0$ . We will carry out an analysis of the roots to the polynomial  $f(z(t))$  with respect to the model weight  $z(t)$ , identifying the number of roots as well as their positions

relative to the minimum  $\bar{z}$ . Note that, as  $z(t)$  is continuous and growing in  $t$  under assumptions (i)-(iv), the analysis is directly translatable to the relative position and number of roots of the polynomial in  $t$ .

First, we observe that  $f(z(t))$  has three distinct real roots if its discriminant

$$\begin{aligned}\Delta_f &= 18a_z b_z c_z d_z - 4a_z c_z^3 - 27a_z^2 d_z^2 + b_z^2 c_z^2 - 4b_z^3 d_z \\ &= -16\lambda^2 \eta^2 \left( 24\gamma^6 \lambda^6 + \gamma^4 \lambda^4 \eta^2 \lambda^{(yx)} (11\rho^2 - 188\rho + 188) \right. \\ &\quad \left. + 16\gamma^2 \lambda^2 \eta^4 \lambda^{(yx)^2} (8\rho^4 - 33\rho^3 + 55\rho^2 - 44\rho + 22) \right. \\ &\quad \left. - 64\eta^6 \lambda^{(yx)^3} (\rho - 1)^2 (\rho^2 - \rho + 1) \right)\end{aligned}$$

is positive, i.e.  $\Delta_f > 0$ . If instead  $\Delta_f = 0$ , then at least two of the roots are the same. In the case  $\Delta_f < 0$ , the polynomial  $f(z(t))$  has only one real root.

We will use *Rouths algorithm* to show that all roots of the polynomial have strictly positive real parts. For a cubic polynomial

$$a_0 x^3 + b_0 x^2 + a_1 + b_1,$$

Rouths algorithm analyses the following table

$$\begin{array}{cc} a_0 & a_1 \\ b_0 & b_1 \\ c_0 & 0 \\ d_0 & 0 \end{array}$$

with

$$\begin{aligned}c_0 &= \frac{b_0 a_1 - b_1 a_0}{b_0}, \\ d_0 &= b_1.\end{aligned}$$

From the table, Rouths theorem states that if  $a_0 > 0$ , then all roots of the polynomial has a strictly negative real part, if and only if the coefficients  $a_0, b_0, c_0, d_0$  are strictly positive. The number of roots with strictly positive real parts is equal to the number of times that the sequence  $a_0, b_0, c_0, d_0$  changes signs.

For the polynomial  $f(z(t))$ , we have

$$\begin{aligned}a_0 &= a_z = 12\lambda^2 \eta^2, \\ b_0 &= b_z = -8\eta^2 \lambda \lambda^{(yx)^{1/2}} (2 - \rho), \\ c_0 &= \frac{b_z c_z - d_z a_z}{b_z} = \frac{\gamma^2 \lambda^2}{2} + 4\eta^2 \lambda^{(yx)} (1 - \rho), \\ d_0 &= d_z = -\gamma^2 \lambda \lambda^{(yx)^{1/2}} (2 - \rho).\end{aligned}$$

We see directly that if  $\gamma, \neq 0, \eta > 0$  and under assumptions (i)-(iv), we have:  $a_0 > 0, b_0 < 0, c_0 > 0, d_0 < 0$ . Hence, the sequence  $a_0, b_0, c_0, d_0$  changes signs

three times, and, following Rouths theorem, the three roots of the polynomial all has strictly positive real parts. Hence, if the roots of  $f(z(t))$  are real, they lie after the point  $z(t) = 0$ .

Note that, for  $\gamma \neq 0, \eta > 0$ , and under assumptions (i)-(iv), the error curve  $\mathcal{L}_{\mathcal{G}}(z(t))$  is convex at  $z(t) = 0$  and  $z(t) = \bar{z}$  (its second derivative is positive at these points), see eq. (20), with an exception for  $\rho = 0$ , where  $\bar{z}$  is instead an undulation point (see appendix A.5). For  $1 \geq \rho > 0$ , we hence must have an even number of inflection points on the interval  $(0, \bar{z})$ . In the case where  $f(z(t))$  has one real root,  $\Delta_f < 0$ , this root, if corresponding to an inflection point, must therefore lie after the point  $\bar{z}$ . In this case, we would have zero inflection points on the interval  $(0, \bar{z})$ . However, if the polynomial has three distinct real roots,  $\Delta_f > 0$ , another possibility is that two, out of the three possible, inflection points lie on the interval  $(0, \bar{z})$ . For  $\rho = 0$ , we observe that one of the three possible roots of the polynomial  $f(z(t))$  is equal to  $z^*$ , and  $\mathcal{L}_{\mathcal{G}}(z(t))$  has a maximum of two inflection points, one on the interval  $(0, \bar{z})$  and one on the interval  $(\bar{z}, z^*)$ , see appendix A.5. We conclude, that for  $\gamma \neq 0, \eta > 0$ , a maximum of two inflection points lie in the interval  $(0, \bar{z})$ .

We investigate, in the case  $\Delta_f > 0$ , and for  $1 \geq \rho > 0$  (we have already concluded that there is a maximum of two inflection points if  $\rho = 0$ ), how many of the three roots of  $f(z(t))$  lies in the interval  $(0, \bar{z})$ . For analysing the relative position of roots of  $f(z(t))$  to the point  $\bar{z}$ , we shift the function  $f(z(t))$  by  $\bar{z}$ , using a change of variables,

$$\begin{aligned} g(x(t)) &= a_x x(t)^3 + b_x x(t)^2 + c_x x(t) + d_x, \\ a_x &= 12\lambda^2 \eta^2, \\ b_x &= -4\eta^2 \lambda \lambda^{(yx)^{1/2}} (7\rho - 5), \\ c_x &= 2(\gamma^2 \lambda^2 + 2\eta^2 \lambda^{(yx)} (5\rho^2 - 7\rho + 2)), \\ d_x &= -\rho \lambda^{(yx)^{1/2}} \left( \gamma^2 \lambda + \frac{4\eta^2 \lambda^{(yx)} (1 - \rho)^2}{\lambda} \right), \end{aligned}$$

with  $x(t) = z(t) - \bar{z}$ , such that  $g(0) = f(\bar{z})$ . Note that  $g(x(t))$  has equally many distinct roots in  $x(t)$  as  $f(z(t))$  has in  $z(t)$ , as shifting the function along the x-axis does not change this fact. Moreover, in the case  $\Delta_f > 0$ , with three real and distinct roots, since all roots of  $f(z(t))$  are strictly positive, the roots of  $g(x(t))$  must be larger than  $-\bar{z}$ .

We evaluate  $g(x(t))$  at the points  $x(t) = -\bar{z}$  (corresponding to  $z(t) = 0$ ) and  $x(t) = 0$  (corresponding to  $z(t) = \bar{z}$ )

$$\begin{aligned} g(-\bar{z}) &= -\gamma^2 \lambda \lambda^{(yx)^{1/2}} (2 - \rho), \\ g(0) &= -\rho \lambda^{(yx)^{1/2}} \left( \gamma^2 \lambda + \frac{4\eta^2 \lambda^{(yx)} (1 - \rho)^2}{\lambda} \right). \end{aligned}$$

Hence, under assumptions (i)-(iv) and with  $\gamma \neq 0, \eta > 0, 1 \geq \rho > 0$ , we have  $g(-\bar{z}), g(0) < 0$ . Now, if we can find a point in the interval  $(-\bar{z}, 0)$  such that  $g(x(t)) > 0$ , then we must conclude that there are at least two roots of  $g(x(t))$



lying on the interval  $(-\bar{z}, 0)$ , and therefore two roots of  $f(z(t))$ , lying on the interval  $(0, \bar{z})$ .

For this purpose, observe that if  $g(x(t))$  has three distinct real roots ( $\Delta_f > 0$ ), then the polynomial must also have two distinct and real local optima, one local minimum and one local maximum lying in between the roots of the polynomial. The local optima are

$$x^\pm = \frac{2\eta\lambda^{(yx)^{1/2}}(7\rho - 5) \pm \sqrt{4\eta^2\lambda^{(yx)}(4\rho^2 - 7\rho + 7) - 18\gamma^2\lambda^2}}{18\eta\lambda}$$

For  $\gamma \neq 0, \eta > 0$ , we have  $a_x > 0$ , and, therefore  $g(x(t)) \rightarrow -\infty$  if  $x(t) \rightarrow -\infty$  and  $g(x(t)) \rightarrow \infty$  if  $x(t) \rightarrow \infty$ , and so the local maximum must be located before the local minimum, i.e. the local maximum is the point

$$x^- = \frac{2\eta\lambda^{(yx)^{1/2}}(7\rho - 5) - \sqrt{4\eta^2\lambda^{(yx)}(4\rho^2 - 7\rho + 7) - 18\gamma^2\lambda^2}}{18\eta\lambda}.$$

Clearly,  $x^- < 0$  if  $5/7 > \rho > 0$ . Note also that in the case of three real and distinct roots, the polynomial  $g(x(t))$  must be positive at the local maximum, i.e.  $g(x^-) > 0$ . Since all of the roots of  $g(x(t))$  are larger than  $-\bar{z}$  and as  $g(-\bar{z}) < 0$ , we therefore also must have  $x^- > -\bar{z}$ . Hence, we have found a point at which  $g(x(t)) > 0$  and that lie on the interval  $(-\bar{z}, 0)$ . Coming back to the original polynomial,  $f(z(t))$ , we conclude that if  $f(z(t))$  has three real and distinct roots and if  $5/7 > \rho > 0$ , then at least two of them must lie in the interval  $(0, \bar{z})$ . Hence, if all of the three roots of  $f(z(t))$  correspond to inflection points in the curve  $\mathcal{L}_G(z(t))$ , as we can have only a maximum of two roots on the interval  $(0, \bar{z})$ , then exactly two of these must lie in the interval  $(0, \bar{z})$ , and the third on the interval  $(\bar{z}, z^*)$ .

**Case  $\gamma \neq 0, \eta = 0$ .** For the one-layer model,  $\eta = 0$ , the polynomial  $f(z(t))$  simplifies to

$$f(z(t)) = 2\gamma^2\lambda^2 z(t) - \gamma^2\lambda\lambda^{(yx)^{1/2}}(2 - \rho).$$

Solving  $f(z(t)) = 0$ , we find

$$\hat{z} = \frac{\lambda^{(yx)^{1/2}}(2 - \rho)}{2\lambda}.$$

Note that for  $\rho = 0$ , we have  $\hat{z} = z^*$ , and, as  $z(t)$  never grows beyond its global minimum  $z^*$ , the error curve  $\mathcal{L}_G(z(t))$  has no inflection points.

For  $1 \geq \rho > 0$ , it is easily verified that

$$1 > \frac{2 - \rho}{2} > 1 - \rho,$$

and therefore  $\hat{z} \in (\bar{z}, z^*)$ . Moreover, for  $\eta = 0, \gamma, \rho > 0$  and under assumptions (i)-(iv), we have

$$\left. \frac{d^2}{dt^2} \mathcal{L}_G(z(t)) \right|_{z(t)=\bar{z}} = 2\gamma^2 \lambda \lambda^{(yx)} \rho^2 > 0.$$

To show that we have a change of convexity at  $\hat{z}$ , we take a point lying on the interval  $(\hat{z}, z^*)$  and evaluate the second derivative of the error at that point:

$$\left. \frac{d^2}{dt^2} \mathcal{L}_G(z(t)) \right|_{z(t)=\frac{\lambda^{(yx)1/2}(2-0.5\rho)}{2\lambda}} = -\frac{\gamma^2 \lambda \lambda^{(yx)} \rho^2}{4} < 0.$$

Hence, under assumptions (i)-(iv), the error curve  $\mathcal{L}_G(z(t))$  is concave beyond the root  $\hat{z}$ , indicating that the point  $\hat{z} \in (\bar{z}, z^*)$  is indeed an inflection point of  $\mathcal{L}_G(z(t))$ . In terms of  $t$ , initialising at  $z(0)$ , this inflection point, using eq. (12), is

$$t(\hat{z}) = \frac{\log\left(\frac{2(\lambda^{(yx)1/2} - \lambda z(0))}{\lambda^{(yx)1/2} \rho}\right)}{|\gamma| \lambda},$$

lying in the interval  $(t^{(1-\rho)z^*}, \infty)$ .

**Case  $\gamma = 0, \eta > 0$ .** For  $\gamma = 0, \eta > 0$ , corresponding to the balanced two-layer dynamics, note that the case  $\rho = 1$  is not covered by assumptions (i)-(iv) and hence we carry out the following analysis for  $1 > \rho \geq 0$ . With  $\gamma = 0$ , the polynomial  $f(z(t))$  simplifies to

$$f(z(t)) = z(t) \left( 12\lambda^2 \eta^2 z(t)^2 - 8\eta^2 \lambda \lambda^{(yx)1/2} (2 - \rho) z(t) + 4\eta^2 \lambda^{(yx)} (1 - \rho) \right).$$

First, we note that the solution  $\hat{z} = 0$  of  $f(z(t)) = 0$  is not an inflection point, as  $z(t) \geq 0$ . To find potential inflection points, we instead solve

$$12\lambda^2 \eta^2 z(t)^2 - 8\eta^2 \lambda \lambda^{(yx)1/2} (2 - \rho) z(t) + 4\eta^2 \lambda^{(yx)} (1 - \rho) = 0,$$

with solutions

$$\hat{z}^\pm = \frac{\lambda^{(yx)1/2} (2 - \rho \pm \sqrt{\rho^2 - \rho + 1})}{3\lambda}.$$

For the first root,  $\hat{z}^-$ , and with  $1 > \rho \geq 0$ , we can verify

$$1 - \rho > \frac{2 - \rho - \sqrt{\rho^2 - \rho + 1}}{3} > 0,$$

and  $\hat{z}^- \in (0, \bar{z})$  for  $1 > \rho \geq 0$ . For the second root,  $\hat{z}^+$ , observe that  $\hat{z}^+ = z^*$  for  $\rho = 0$ , and hence,  $\hat{z}^+$  is not an inflection point for  $\rho = 0$ . For  $1 \geq \rho > 0$ , we find

$$1 > \frac{2 - \rho + \sqrt{\rho^2 - \rho + 1}}{3} > 1 - \rho,$$

and, hence,  $\hat{z}^+ \in (\bar{z}, z^*)$  for  $1 \geq \rho > 0$ . To verify the convexity of  $\mathcal{L}_{\mathcal{G}}(z(t))$  between the roots  $\hat{z}^-$ ,  $\hat{z}^+$ , we take a point on the interval  $(\hat{z}^-, \hat{z}^+)$  and evaluate the second derivative at this point

$$\left. \frac{d^2}{dt^2} \mathcal{L}_{\mathcal{G}}(z(t)) \right|_{z(t) = \frac{\lambda^{(yx)^{1/2}(2-\rho)}}{3\lambda}} = \frac{8\eta^2 \lambda^{(yx)^2} (\rho-2)(\rho+1)(\rho^2 - \rho + 1)}{27\lambda} > 0.$$

In other words,  $\mathcal{L}_{\mathcal{G}}(z(t))$  is convex in between the roots.

Moreover, we observe that the error curve is concave outside of the interval  $(\hat{z}^-, \hat{z}^+)$ . First consider the case  $1 > \rho > 0$ . We can use the upper bound  $1 > \sqrt{1 - \rho + \rho^2}$  to find a point lying on the interval  $(0, \hat{z}^-)$ , for which the second derivative of  $\mathcal{L}_{\mathcal{G}}(z(t))$  is negative

$$\left. \frac{d^2}{dt^2} \mathcal{L}_{\mathcal{G}}(z(t)) \right|_{z(t) = \frac{\lambda^{(yx)^{1/2}(1-\rho)}}{3\lambda}} = -\frac{8\eta^2 \lambda^{(yx)^2} \rho(1-\rho)^2(\rho+2)}{27\lambda} < 0.$$

Similarly, we find a point lying on the interval  $(\hat{z}^+, z^*)$ , for which

$$\left. \frac{d^2}{dt^2} \mathcal{L}_{\mathcal{G}}(z(t)) \right|_{z(t) = \frac{\lambda^{(yx)^{1/2}(3-\rho)}}{3\lambda}} = -\frac{8\eta^2 \lambda^{(yx)^2} \rho^2(\rho-1)(\rho-3)}{27\lambda} < 0.$$

Hence with  $\gamma = 0, \eta > 0$  and for  $1 > \rho > 0$  and under assumptions (iv)-(iv), the error curve  $\mathcal{L}_{\mathcal{G}}(z(t))$  has two inflection points:  $\hat{z}^- \in (0, \bar{z})$  and  $\hat{z}^+ \in (\bar{z}, \infty)$ .

For  $\rho = 0$ , we have only one root of  $f(z(t))$  lying in the interval  $(0, z^*)$ :

$$\hat{z}^- = \frac{\lambda^{(yx)^{1/2}}}{3\lambda}.$$

We have shown already that, for  $\rho = 0$ , the error curve  $\mathcal{L}_{\mathcal{G}}(z(t))$  is convex at a point in the interval  $(\hat{z}^-, z^*)$  (see the evaluation of the second derivative at  $z(t) = \lambda^{(yx)^{1/2}(2-\rho)}/(3\lambda)$ ). To show that  $\hat{z}^-$  is an inflection point we additionally evaluate the second derivative of  $\mathcal{L}_{\mathcal{G}}(z(t))$  at a point in the interval  $(0, \hat{z}^-)$ :

$$\left. \frac{d^2}{dt^2} \mathcal{L}_{\mathcal{G}}(z(t)) \right|_{z(t) = \frac{\lambda^{(yx)^{1/2}}}{4\lambda}} = -\frac{9\eta^2 \lambda^{(yx)^2}}{32\lambda} < 0.$$

Hence, with  $\gamma = 0, \eta > 0$ , and for  $\rho = 0$ , the error curve  $\mathcal{L}_{\mathcal{G}}(z(t))$  has one inflection point at  $\hat{z}^- \in (0, \bar{z})$ .

In terms of  $t$ , initialising at  $z(0)$  the inflection points  $\hat{z}^{\pm}$ , using eq. (12), translates to

$$t(\hat{z}^{\pm}) = \frac{\log \left( \frac{(\lambda^{(yx)^{1/2}} - \lambda z(0))(1 \pm \sqrt{\rho^2 - \rho + 1})}{\lambda \rho z(0)} \right)}{2\eta \lambda^{(yx)^{1/2}}},$$

if  $1 > \rho > 0$ . If  $\rho = 0$ , we have

$$t(\hat{z}^-) = \frac{\log\left(\frac{\lambda^{(yx)1/2} - \lambda z(0)}{2\lambda z(0)}\right)}{2\eta\lambda^{(yx)1/2}}.$$

The inflection point  $t(\hat{z}^-)$  will lie in the interval  $(0, t^{(1-\rho)z^*})$  if  $z(0) < \hat{z}^-$ , and will otherwise either lie at 0 ( $z(0) = \hat{z}^-$ ), corresponding to an undulation point and not an inflection point, or lie outside of the interval  $(0, t^{(1-\rho)z^*})$  ( $z(0) > \hat{z}^-$ ), for which the inflection point will not exist. Meanwhile,  $t(\hat{z}^+)$  will lie in the interval  $(t^{(1-\rho)z^*}, \infty)$ .

In summary, we conclude that, under assumptions (i)-(iv), the error curve  $\mathcal{L}_{\mathcal{G}}(z(t))$  has a maximum of three inflection points, whereof a maximum of two lies in the interval  $(0, \bar{z})$ . If three inflection points exist and  $5/7 > \rho > 0$ , then two inflection points lie in the interval  $(0, \bar{z})$  and one in the interval  $(\bar{z}, z^*)$ . Under assumptions (i)-(iv), we note that  $z(t)$  is continuous as well as growing in time,  $t$ , and hence the conclusions are directly transferable to the corresponding inflection points in terms of  $t$ , replacing  $\bar{z}$  with  $t(\bar{z}) = t^{(1-\rho)z^*}$  and  $z^*$  with  $t(z^*) = \infty$ . Indeed, we can have  $z(0) > 0$ , and it is therefore possible that there is a fewer number of inflection points on the time interval  $(0, \infty)$  compared to the variable interval  $(0, z^*)$ . However, note that the conclusions still hold, referring to a maximum number of inflection points, or being contingent on having exactly three inflection points. This ends the proof of lemma 2.

## A.7 Proof of proposition 3 and corollary 1

To prove proposition 3 and corollary 1, we consider the weight matrix  $Z(t)$  with  $|S_{\mathcal{A}}|$  active weights, following eq. (6). The total generalisation error, eq. (10), is a sum over  $|S_{\mathcal{A}}|$  error curves. We show that, under assumptions (i)-(iv), a necessary condition for this generalisation error to exhibit a double descent pattern over the course of learning, is that we can find at least one inflection point,  $\hat{t}$ , belonging to either one of the  $|S_{\mathcal{A}}|$  individual error curves, such that

$$\min\{t_i^{(1-\rho_i)z_i^*}; i \in S_{\mathcal{A}}\} < \hat{t} < \max\{t_i^{(1-\rho_i)z_i^*}; i \in S_{\mathcal{A}}\}.$$

We prove this necessary condition by showing that if there is no inflection point  $\hat{t}$  lying in the interval  $(\min\{t_i^{(1-\rho_i)z_i^*}; i \in S_{\mathcal{A}}\}, \max\{t_i^{(1-\rho_i)z_i^*}; i \in S_{\mathcal{A}}\})$ , then the error curve  $\mathcal{L}_{\mathcal{G}}(Z(t))$  does *not* exhibit a double descent pattern.

We first observe that double descent requires that the error curve  $\mathcal{L}_{\mathcal{G}}(Z(t))$  declines in  $t$ , i.e.

$$\frac{d}{dt}\mathcal{L}_{\mathcal{G}}(Z(t)) < 0,$$

at a time interval succeeding an interval for which  $\mathcal{L}_{\mathcal{G}}(Z(t))$  grows in  $t$ , i.e.

$$\frac{d}{dt}\mathcal{L}_{\mathcal{G}}(Z(t)) > 0.$$

We show that this is not possible if there is no  $\hat{t}$  lying in the interval  $(\min\{t_i^{(1-\rho_i)z_i^*}; i \in S_{\mathcal{A}}\}, \max\{t_i^{(1-\rho_i)z_i^*}; i \in S_{\mathcal{A}}\})$ .

First, observe that in the time interval  $[0, \min\{t_i^{(1-\rho_i)z_i^*}; i \in S_{\mathcal{A}}\}]$ , all individual error curves  $\mathcal{L}_{\mathcal{G}}(z_i(t))$ ,  $i \in S_{\mathcal{A}}$ , are decreasing or constant in  $t$ , i.e.

$$\frac{d}{dt}\mathcal{L}_{\mathcal{G}}(z_i(t)) \leq 0, \forall i \in S_{\mathcal{A}},$$

and so

$$\frac{d}{dt}\mathcal{L}_{\mathcal{G}}(Z(t)) \leq 0,$$

following eq. (10). In addition, in the interval  $[\max\{t_i^{(1-\rho_i)z_i^*}; i \in S_{\mathcal{A}}\}, \infty)$ , we have

$$\frac{d}{dt}\mathcal{L}_{\mathcal{G}}(z_i(t)) \geq 0, \forall i \in S_{\mathcal{A}},$$

and therefore

$$\frac{d}{dt}\mathcal{L}_{\mathcal{G}}(Z(t)) \geq 0.$$

To determine the behaviour of the generalisation error in between the two points  $\min\{t_i^{(1-\rho_i)z_i^*}; i \in S_{\mathcal{A}}\}$  and  $\max\{t_i^{(1-\rho_i)z_i^*}; i \in S_{\mathcal{A}}\}$ , we observe that under assumptions (i)-(iv) and following lemma 1, each individual error curve  $\mathcal{L}_{\mathcal{G}}(z_i(t))$ ,  $i \in S_{\mathcal{A}}$ , for which  $1 \geq \rho_i > 0$ , is convex at  $\bar{z}$ . We point out that for  $\rho_i = 1$ , we have  $\bar{z}_i = 0$ , and hence, under assumptions (i)-(iv),  $z_i(t)$  must begin at the point  $\bar{z}$ , so the error curve will be convex to start. For  $\rho_i = 0$ , again following lemma 1, the curve is convex leading up to the minimum, at which point the second derivative of  $\mathcal{L}_{\mathcal{G}}(z_i(t))$  is 0, and after which  $z_i(t)$  will remain constant (note, however, that this happens at  $t \rightarrow \infty$ ).

Taken together, if there is no inflection point  $\hat{t}$ , belonging to either one of the individual error curves  $\mathcal{L}_{\mathcal{G}}(z_i(t))$ ,  $i \in S_{\mathcal{A}}$ , and lying in the interval  $(\min\{t_i^{(1-\rho_i)z_i^*}; i \in S_{\mathcal{A}}\}, \max\{t_i^{(1-\rho_i)z_i^*}; i \in S_{\mathcal{A}}\})$ , then, on this interval, we must have

$$\frac{d^2}{dt^2}\mathcal{L}_{\mathcal{G}}(z_i(t)) \geq 0, \forall i \in S_{\mathcal{A}},$$

and, therefore,

$$\frac{d^2}{dt^2}\mathcal{L}_{\mathcal{G}}(Z(t)) \geq 0.$$

Now, assuming that there are no inflection points on the interval  $(\min\{t_i^{(1-\rho_i)z_i^*}; i \in S_{\mathcal{A}}\}, \max\{t_i^{(1-\rho_i)z_i^*}; i \in S_{\mathcal{A}}\})$ , take any time point  $t'$  for which

$$\left.\frac{d}{dt}\mathcal{L}_{\mathcal{G}}(Z(t))\right|_{t=t'} > 0,$$

i.e., the error curve  $\mathcal{L}_{\mathcal{G}}(Z(t))$  is growing at time  $t'$ . Note that, by the previous statements made regarding the first and second time derivatives of  $\mathcal{L}_{\mathcal{G}}(Z(t))$ , we must have  $t' \in (\min\{t_i^{(1-\rho_i)z_i^*}; i \in S_{\mathcal{A}}\}, \infty)$ . Then, take any other time point  $t''$  such that  $t'' > t'$ . Either  $t'' \in (\min\{t_i^{(1-\rho_i)z_i^*}; i \in S_{\mathcal{A}}\}, \max\{t_i^{(1-\rho_i)z_i^*}; i \in S_{\mathcal{A}}\})$ , for which it must hold that, as  $\mathcal{L}_{\mathcal{G}}(Z(t))$  is convex on the interval,

$$\frac{d}{dt}\mathcal{L}_{\mathcal{G}}(Z(t))\Big|_{t=t''} \geq \frac{d}{dt}\mathcal{L}_{\mathcal{G}}(Z(t))\Big|_{t=t'} > 0,$$

or  $t'' \in [\max\{t_i^{(1-\rho_i)z_i^*}; i \in S_{\mathcal{A}}\}, \infty)$ , for which

$$\frac{d}{dt}\mathcal{L}_{\mathcal{G}}(Z(t))\Big|_{t=t''} \geq 0.$$

We can conclude that there is no time point  $t''$ , following a time point  $t'$  at which  $\mathcal{L}_{\mathcal{G}}(Z(t))$  is growing in  $t$ , such that

$$\frac{d}{dt}\mathcal{L}_{\mathcal{G}}(Z(t))\Big|_{t=t''} < 0.$$

Therefore, the error curve  $\mathcal{L}_{\mathcal{G}}(Z(t))$  will not exhibit a double descent pattern.

On the other hand, if there is an inflection point  $\hat{t} \in (\min\{t_i^{(1-\rho_i)z_i^*}; i \in S_{\mathcal{A}}\}, \max\{t_i^{(1-\rho_i)z_i^*}; i \in S_{\mathcal{A}}\})$ , belonging to either of the individual error curves  $\mathcal{L}_{\mathcal{G}}(z_i(t))$ ,  $i \in S_{\mathcal{A}}$ , there will be at least one sub-interval of  $(\min\{t_i^{(1-\rho_i)z_i^*}; i \in S_{\mathcal{A}}\}, \max\{t_i^{(1-\rho_i)z_i^*}; i \in S_{\mathcal{A}}\})$ , where it holds for at least one  $z_i(t)$ ,  $i \in S_{\mathcal{A}}$ , that

$$\frac{d^2}{dt^2}\mathcal{L}_{\mathcal{G}}(z_i(t)) < 0.$$

Hence, the error curve  $\mathcal{L}_{\mathcal{G}}(Z(t))$  possibly exhibits a non-convex behaviour on the interval  $(\min\{t_i^{(1-\rho_i)z_i^*}; i \in S_{\mathcal{A}}\}, \max\{t_i^{(1-\rho_i)z_i^*}; i \in S_{\mathcal{A}}\})$ , potentially giving rise to a double descent pattern. This concludes the proof of proposition 3.

For the proof of corollary 1, consider the special case with two active weights,  $z_i(t), z_j(t)$ . From the assumption  $t_i^{(1-\rho_i)z_i^*} < t_j^{(1-\rho_j)z_j^*}$ , it follows directly that

$$\begin{aligned} \min\{t_i^{(1-\rho_i)z_i^*}; i \in S_{\mathcal{A}}\} &= t_i^{(1-\rho_i)z_i^*}, \\ \max\{t_i^{(1-\rho_i)z_i^*}; i \in S_{\mathcal{A}}\} &= t_j^{(1-\rho_j)z_j^*}. \end{aligned}$$

Hence, the necessary condition for observing double descent simplifies to having at least one inflection point  $\hat{t}$ , belonging to either of the error curves  $\mathcal{L}_{\mathcal{G}}(z_i(t))$  and  $\mathcal{L}_{\mathcal{G}}(z_j(t))$ , with

$$t_i^{(1-\rho_i)z_i^*} < \hat{t} < t_j^{(1-\rho_j)z_j^*}.$$

Now, provided that it exists, let  $\hat{t}_j^-$  denote the maximum inflection point belonging to the second curve,  $\mathcal{L}_{\mathcal{G}}(z_j(t))$ , lying in the interval  $(0, t_j^{(1-\rho_j)z_j^*})$ . Moreover,

let, provided that it exists,  $\hat{t}_i^+$  denote the minimum inflection point belonging to the first error curve,  $\mathcal{L}_{\mathcal{G}}(z_i(t))$ , and lying on the interval  $(t_i^{(1-\rho_i)z_i^*}, \infty)$ . We note that we only need to consider the maximum inflection point on the interval  $(0, t_j^{(1-\rho_j)z_j^*})$  belonging to the curve  $\mathcal{L}_{\mathcal{G}}(z_j(t))$ , as if a smaller inflection point exists on the same interval and this inflection point also lies in the interval  $(t_i^{(1-\rho_i)z_i^*}, t_j^{(1-\rho_j)z_j^*})$ , so must  $\hat{t}_i^+$ . In a similar manner, we only need to consider the minimum inflection point on the interval  $(t_i^{(1-\rho_i)z_i^*}, \infty)$ , belonging to the curve  $\mathcal{L}_{\mathcal{G}}(z_i(t))$ , as if a larger inflection point exists on this interval and also lies in the interval  $(t_i^{(1-\rho_i)z_i^*}, t_j^{(1-\rho_j)z_j^*})$ , so must  $\hat{t}_i^+$ . Then, a necessary condition for double descent, following the condition above, is that at least one of the two inflection points  $\hat{t}_i^+$  and  $\hat{t}_j^-$  lies in the interval  $(t_i^{(1-\rho_i)z_i^*}, t_j^{(1-\rho_j)z_j^*})$ , which can be equivalently written as fulfilling one of

$$\begin{aligned} t_i^{(1-\rho_i)z_i^*} &< \hat{t}_j^-, \\ \hat{t}_i^+ &< t_j^{(1-\rho_j)z_j^*}. \end{aligned}$$

Note that assuming  $t_i^{(1-\rho_i)z_i^*} < t_j^{(1-\rho_j)z_j^*}$  is without loss of generality. If the opposite holds, just change the order of  $z_i(t)$  and  $z_j(t)$ . This concludes the proof of corollary 1.

## A.8 Derivation of train MSE

We derive eq. (15), the train MSE in terms of the weight matrix  $Z(t) = U^{(yx)\top} W(t) V^{(yx)}$ , starting from eq. (1). As previously, let  $n^{-1/2} \mathbf{X} = U \Sigma^{1/2} V^\top$  and  $n^{-1} \mathbf{y}^\top \mathbf{X} = U^{(yx)} \Sigma^{(yx)1/2} V^\top$ . Then,

$$\begin{aligned} \mathcal{L}_{\mathcal{G}}(Z(t)) &= \frac{1}{2n} \text{Tr} \left( (\mathbf{y} - \mathbf{X}(U^{(yx)} Z(t) V^\top)^\top)^\top (\mathbf{y} - \mathbf{X}(U^{(yx)} Z(t) V^\top)^\top) \right) \\ &= \frac{1}{2n} \text{Tr} \left( (\mathbf{y} - \mathbf{X} V Z^*{}^\top U^{(yx)\top} + \mathbf{X} V Z^*{}^\top U^{(yx)\top} - \mathbf{X} V Z(t)^\top U^{(yx)\top})^\top \right. \\ &\quad \left. (\mathbf{y} - \mathbf{X} V Z^*{}^\top U^{(yx)\top} + \mathbf{X} V Z^*{}^\top U^{(yx)\top} - \mathbf{X} V Z(t)^\top U^{(yx)\top}) \right) \\ &= \frac{1}{2n} \text{Tr} \left( (\epsilon + \mathbf{X} V (Z^* - Z(t))^\top U^{(yx)\top})^\top (\epsilon + \mathbf{X} V (Z^* - Z(t))^\top U^{(yx)\top}) \right) \\ &= \frac{1}{2n} \text{Tr} \left( (\epsilon^\top \epsilon + 2\epsilon^\top \mathbf{X} V (Z^* - Z(t))^\top U^{(yx)\top} \right. \\ &\quad \left. + U^{(yx)} (Z^* - Z(t)) V^\top \mathbf{X}^\top \mathbf{X} V (Z^* - Z(t))^\top U^{(yx)\top} \right) \\ &\stackrel{(1)}{=} \frac{1}{2} \text{Tr} \left( U^{(yx)} (\Sigma^{(yx)} \Sigma^\dagger - Z(t)) \Sigma (\Sigma^{(yx)} \Sigma^\dagger - Z(t))^\top U^{(yx)\top} + \epsilon^\top \epsilon \right) \\ &= \frac{1}{2} \text{Tr} \left( (\Sigma^{(yx)} \Sigma^\dagger - Z(t)) \Sigma (\Sigma^{(yx)} \Sigma^\dagger - Z(t))^\top + \epsilon^\top \epsilon \right) \\ &= \frac{1}{2} \sum_{i \in S_{\mathcal{A}}} \lambda_i (\lambda^{(yx)1/2} \lambda^{-1} - z_i(t))^2 + \text{const.}, \end{aligned}$$

with the sum being over  $i \in S_{\mathcal{A}}$ , the indices of the active weights in  $Z(t)$ , while the constant term includes possible constant error corresponding to inactive elements in  $Z(t)$  as well as the residual error of the global minimum  $Z^* = \Sigma^{(yx)}\Sigma^\dagger$ . In (1) we rewrite

$$\begin{aligned} 2\epsilon^\top \mathbf{X}V(Z^* - Z)^\top U^{(yx)\top} &= 2(\mathbf{y}^\top \mathbf{X} - U^{(yx)}Z^*V^\top \mathbf{X}^\top \mathbf{X})V(Z^* - Z)^\top U^{(yx)\top} \\ &= 2n^{-1}U^{(yx)}(\Sigma^{(yx)1/2} - Z^*\Sigma)(Z^* - Z)^\top U^{(yx)\top} \\ &= 0, \end{aligned}$$

contingent on  $\text{rank}(\Sigma) \geq \text{rank}(\Sigma^{(yx)1/2})$ . We recover eq. (15) by replacing  $z^* = \lambda^{(yx)1/2}\lambda^{-1}$ .

### A.8.1 Convexity of train MSE with $\eta = 0$

To see that the training loss, eq. (15), is convex in  $t$  for the one-layer model ( $\eta = 0$ ), consider the error term of a single weight  $z_i(t)$

$$\mathcal{L}(z_i(t)) = \lambda_i(z_i^* - z_i(t))^2$$

as part of the sum in eq. (15). For  $z_i(t)$  following eq. (7), the first and second time derivatives of  $\mathcal{L}(z_i(t))$  are

$$\begin{aligned} \frac{d}{dt}\mathcal{L}(z_i(t)) &= -2|\gamma|(z_i^* - \lambda_i z_i(t))^2, \\ \frac{d^2}{dt^2}\mathcal{L}(z_i(t)) &= 4\gamma^2\lambda_i(z_i^* - \lambda_i z_i(t))^2. \end{aligned}$$

We see immediately that, under assumptions (i)-(iv),

$$\frac{d^2}{dt^2}\mathcal{L}(z_i(t)) \geq 0,$$

and  $\mathcal{L}(z_i(t))$  is convex in  $t$ . Being a sum over convex curves, the total training loss in eq. (15) must also be convex in  $t$ .

## A.9 Deep linear models

We derive the approximate dynamics of decoupled multi-layer linear neural networks, eq. (16), and identify inflection points in the error curve eq. (11) with  $z_i(t)$  following the derived dynamics.

### A.9.1 Derivation of dynamics for deep linear model

To derive the multi-layer dynamics in eq. (16), we start from the linear model of  $L$  layers

$$\begin{aligned} \hat{y} &= xW^\top, \\ W &= \prod_{\ell=1}^L W^{(\ell)}, \end{aligned}$$



with weight matrices  $W^{(\ell)} \in \mathbb{R}^{h^{(\ell)} \times h^{(\ell-1)}}$ , and where  $h^{(0)} = d$  and  $h^{(L)} = d_y$ . Gradients of the MSE loss, eq. (1), are

$$\frac{1}{\eta_\ell} \frac{d}{dt} W^{(\ell)} = \frac{1}{n} \left( \prod_{j=\ell+1}^L W^{(j)} \right)^\top (\mathbf{y}^\top \mathbf{X} - W \mathbf{X}^\top \mathbf{X}) \left( \prod_{j=1}^{\ell-1} W^{(j)} \right)^\top,$$

with  $\eta_\ell \geq 0$  the learning rate of layer  $\ell$  and where we assume  $\prod_{j=\ell_l}^{\ell_u} W^{(j)} = \mathbb{I}$  (the identity matrix) if  $\ell_l > \ell_u$ .

We follow [20] and initialise weight matrices as  $W^{(\ell)}(0) = R^{(\ell+1)} D^{(\ell)} R^{(\ell)\top}$ , where  $R^{(\ell)}$ ,  $\ell = 1, 2, \dots, L$ , are orthogonal matrices, with  $R^{(1)} = V$  and  $R^{(L)} = U^{(yx)}$ , and  $D^{(\ell)}$ ,  $\ell = 1, 2, \dots, L$ , are diagonal matrices. The synaptic weights  $Z^{(\ell)} = R^{(\ell+1)\top} W^{(\ell)} R^{(\ell)}$ , using the SVDs of  $\mathbf{X}$  and  $\mathbf{y}^\top \mathbf{X}$ , then evolve as

$$\frac{1}{\eta_\ell} \frac{d}{dt} Z^{(\ell)} = \left( \prod_{j=\ell+1}^L Z^{(j)} \right)^\top (\Sigma^{(yx)1/2} - Z \Sigma) \left( \prod_{j=1}^{\ell-1} Z^{(j)} \right)^\top.$$

Observe that, with the given initialisation,  $Z^{(\ell)}(0)$ ,  $\ell = 1, 2, \dots, L$ , is diagonal, and the gradients of any non-diagonal elements will be zero. Following this, each weight matrix  $Z^{(\ell)}(t)$  will remain diagonal throughout the course of learning. The gradient of the  $i^{\text{th}}$  diagonal element of layer  $\ell$ , denoted  $a_i^{(\ell)}$ , is

$$\frac{1}{\eta_\ell} \frac{da_i^{(\ell)}}{dt} = \prod_{j \neq \ell} a_i^{(j)} \left( \lambda_i^{(yx)1/2} - \lambda_i \prod_{j=1}^L a_i^{(j)} \right),$$

with  $\lambda_i, \lambda_i^{(yx)1/2}$  the  $i^{\text{th}}$  diagonal elements of  $\Sigma, \Sigma^{(yx)1/2}$ , respectively.

Similar to [20] and the two layer dynamics in eq. (5), these dynamics exhibit conserved quantities in the form of  $\eta_j a_i^{(\ell)2} - \eta_\ell a_i^{(j)2} = \gamma_{\ell,j} \forall \ell, j \in \{1, \dots, L\}$ . We can easily verify

$$\frac{d}{dt} (\eta_j a_i^{(\ell)2} - \eta_\ell a_i^{(j)2}) = 2\eta_j a_i^{(\ell)} \frac{da_i^{(\ell)}}{dt} - 2\eta_\ell a_i^{(j)} \frac{da_i^{(j)}}{dt} = 0.$$

We use this to rewrite the gradient dynamics for the  $i^{\text{th}}$  diagonal element,  $z_i = \prod_{j=1}^L a_i^{(j)}$ , of the full weight matrix  $Z$

$$\begin{aligned} \frac{dz_i}{dt} &= \sum_{j=1}^L \eta_j \prod_{k \neq j} a_i^{(k)2} (\lambda_i^{(yx)1/2} - \lambda_i z_i) \\ &= \sum_{j=1}^L \eta_j \prod_{k \neq j} \frac{\gamma_{k,L} + \eta_k a_i^{(L)2}}{\eta_L} (\lambda_i^{(yx)1/2} - \lambda_i z_i). \end{aligned}$$

To simplify the dynamics further, we assume  $L$  even, and group parameters in two groups, with  $\gamma_{j,L} = \gamma$ ,  $\eta_j = \eta_1$ , for  $j = 1, \dots, L/2$ , and  $\gamma_{j,L} = 0$ ,  $\eta_j = \eta_L$ , for  $j = L/2 + 1, \dots, L$ . Then,

$$z_i = \prod_{j=1}^L a_i^{(j)} = \pm \left( \sqrt{\frac{\gamma + \eta_1 a_i^{(L)^2}}{\eta_L}} \right)^{L/2} \left( \sqrt{a_i^{(L)^2}} \right)^{L/2},$$

from which we find

$$a_i^{(L)^2} = \frac{-\gamma + \sqrt{\gamma^2 + 4\eta_1\eta_L z_i^{4/L}}}{2\eta_1}.$$

Inserting this into the dynamics of  $z_i$  and simplifying, we obtain

$$\frac{dz_i}{dt} = \frac{L}{2} \sqrt{\gamma^2 + 4\eta_1\eta_L z_i^{4/L}} z_i^{2(1-2/L)} (\lambda_i^{(yx)^{1/2}} - \lambda_i z_i).$$

For large  $L$ , we have

$$\frac{dz_i}{dt} \approx \frac{L}{2} |\gamma| z_i^2 (\lambda_i^{(yx)^{1/2}} - \lambda_i z_i),$$

recovering eq. (16).

### A.9.2 Generalisation error of deep linear models

Assuming that the true model is linear, eq. (9), we note that we can rewrite the generalisation error of the multi-layer linear model, eq. (16), just as for the two-layer linear model, as a sum over individual error curves, eq. (10). To understand the behaviour of the generalisation error of the weight matrix  $Z(t)$  with weights following the decoupled dynamics of eq. (16), we analyse the behaviour of the error curve in eq. (11), under assumptions (iv)-(iv) and provided that  $\gamma \neq 0$ ,  $z_i(0) \neq 0$ . The purpose of the two latter assumptions is to ensure that  $z_i(t)$  is growing in  $t$ , and to avoid scenarios in which  $z_i(t)$  diverges. Observe that if  $\gamma = 0$  or  $z(0) = 0$ ,  $z(t)$  will be constant.

We analyse the shape of eq. (11), by identifying its inflection points. First, from eq. (16), we have

$$\frac{d^2 z}{dt^2} = \frac{1}{2} L^2 \gamma^2 z^3 (\lambda^{(yx)^{1/2}} - \lambda z) (\lambda^{(yx)^{1/2}} - \frac{3}{2} \lambda z),$$

dropping all subscripts  $i$ . The first and second time derivatives of the error curve in eq. (11) with  $z(t)$  following eq. (16) are

$$\begin{aligned} \frac{d\mathcal{L}_{\mathcal{G}}(z(t))}{dt} &= -L |\gamma| z(t)^2 ((1 - \rho) \lambda^{(yx)^{1/2}} - \lambda z(t)) (\lambda^{(yx)^{1/2}} - \lambda z(t)), \\ \frac{d^2 \mathcal{L}_{\mathcal{G}}(z(t))}{dt^2} &= -\frac{1}{2} L^2 \gamma^2 z(t)^3 (\lambda^{(yx)^{1/2}} - \lambda z(t)) \\ &\quad \cdot (4\lambda^2 z(t)^2 - 3\lambda \lambda^{(yx)^{1/2}} (2 - \rho) z(t) + 2\lambda^{(yx)} (1 - \rho)) \end{aligned}$$

We point out that with  $z_i(t)$ ,  $i \in S_{\mathcal{A}}$ , growing in  $t$ , the error curve in eq. (11), for each weight  $z_i(t)$ , will be either monotonically decreasing, U-shaped or monotonically increasing in  $t$ . We can see this by noting that under assumptions (i)-(iv) and with  $\gamma \neq 0$ ,  $z(0) \neq 0$ ,

$$(\lambda^{(yx)^{1/2}} - \lambda z(t)) \geq 0, \forall t.$$

Therefore, the first time derivative of  $\mathcal{L}_{\mathcal{G}}(z(t))$  changes signs only at one point, namely at  $z(t) = \bar{z}$ . If  $\bar{z} \geq z^*$  or  $\bar{z} \leq z(0)$ , this point is never passed, and the error curve  $\mathcal{L}_{\mathcal{G}}(z(t))$  is monotonically decreasing or increasing in  $t$ , respectively. If  $z^* > \bar{z} > z(0)$ , the point  $\bar{z}$  is passed once, and the error curve  $\mathcal{L}_{\mathcal{G}}(z(t))$  is U-shaped. Therefore, epoch-wise double descent in the decoupled multi-layer model, if it appears, is a result of a superposition of monotonically decreasing, U-shaped or monotonically increasing curves.

Next, we find potential inflection points of the error curve  $\mathcal{L}_{\mathcal{G}}(z(t))$  by solving

$$\frac{d^2 \mathcal{L}_{\mathcal{G}}(z(t))}{dt^2} = 0.$$

Solutions to this equation include  $z(t) = 0$  and  $z(t) = z^*$ , none of which are inflection points, as  $z(t) \in [0, z^*]$ . The other two solutions are

$$\hat{z}^{\pm} = \frac{\lambda^{(yx)^{1/2}} (6 - 3\rho \pm \sqrt{9\rho^2 - 4\rho + 4})}{8\lambda}$$

We can verify, under assumptions (i)-(iv) and  $\gamma \neq 0$ ,  $z(0) \neq 0$ , that for  $1 > \rho \geq 0$

$$1 - \rho > \frac{6 - 3\rho - \sqrt{9\rho^2 - 4\rho + 4}}{8} > 0,$$

and so  $\hat{z}^- \in (0, \bar{z})$ . We can also verify, for  $1 > \rho > 0$

$$1 > \frac{6 - 3\rho + \sqrt{9\rho^2 - 4\rho + 4}}{8} > 1 - \rho,$$

and so  $\hat{z}^+ \in (\bar{z}, z^*)$ . Note that we exclude the case  $\rho = 1$ , as it under assumptions (i)-(iv) would require  $z(0) = 0$ , contradicting the assumption  $z(0) > 0$ . We evaluate the second derivative at a point in between the two roots

$$\left. \frac{d^2}{dt^2} \mathcal{L}_{\mathcal{G}}(z(t)) \right|_{z(t) = \frac{3(2-\rho)\lambda^{(yx)^{1/2}}}{8\lambda}} = - \frac{27L^2\gamma^2\lambda^{(yx)^3}(\rho-2)^3(3\rho+2)(9\rho^2-4\rho+4)}{131072\lambda^3} > 0,$$

finding that the error curve  $\mathcal{L}_{\mathcal{G}}(z(t))$  is convex in between the roots  $\hat{z}^-$  and  $\hat{z}^+$ . For  $1 > \rho \geq 0$ , we evaluate the second derivative at a point in the interval  $(0, \hat{z}^-)$

$$\left. \frac{d^2}{dt^2} \mathcal{L}_{\mathcal{G}}(z(t)) \right|_{z(t) = \frac{3(1-\rho)\lambda^{(yx)^{1/2}}}{8\lambda}} = - \frac{27L^2\gamma^2\lambda^{(yx)^3}(\rho-1)^4(3\rho+5)(9\rho+5)}{131072\lambda^3} < 0,$$

and, for  $1 > \rho > 0$ , at a point in the interval  $(\hat{z}^+, z^*)$

$$\frac{d^2}{dt^2} \mathcal{L}g(z(t)) \Big|_{z(t) = \frac{(8-\rho)\lambda^{(yx)^{1/2}}}{8\lambda}} = -\frac{L^2\gamma^2\lambda^{(yx)^3}\rho^2(\rho-8)^3(5\rho-12)}{131072\lambda^3} < 0,$$

provided that our assumptions hold. Hence, we find that the curve changes convexity around the roots  $\hat{z}^\pm$ , and that they indeed are inflection points under the given restrictions on  $\rho$ , with  $\hat{z}^- \in (0, \bar{z})$  if  $1 > \rho \geq 0$  and  $\hat{z}^+ \in (\bar{z}, z^*)$  if  $1 > \rho > 0$ . Note that under assumptions (i)-(iv) with  $\gamma \neq 0$  and  $z(0) \neq 0$ , a weight  $z(t)$  following the dynamics eq. (16) will monotonically increase in  $t$ . Hence, the inflection points  $\hat{z}^\pm$  will correspond to unique time points  $\hat{t}^\pm$ , for  $t^-$  provided that  $z(0) < \hat{z}^-$ . To conclude, under assumptions (i)-(iv) with  $\gamma \neq 0$  and  $z(0) \neq 0$ , if  $z(0) < \hat{z}^-$  and  $1 > \rho \geq 0$ , the first inflection point,  $\hat{t}^-$ , will lie in the interval  $(0, t^{(1-\rho)z^*})$ . Moreover, if  $1 > \rho > 0$ , there will be a second inflection point, lying in the interval  $(t^{(1-\rho)z^*}, \infty)$ .